Pathological slow-wave activity and impaired working memory binding in post-traumatic amnesia

EEG changes in post-traumatic amnesia

Emma-Jane Mallas,[1,2] Nikos Gorgoraptis,[1] Sophie Dautricourt,[3] Yoni Pertzov,[4] Gregory Scott[1,2,†] and David J. Sharp [1,2,5,†]

†These authors contributed equally to this work.

[1] Department of Brain Sciences, Imperial College London, London, UK

[2] UK Dementia Research Institute, Care Research and Technology Centre, Imperial College London, London, UK

[3] Inserm UMR-S U1237, Caen-Normandie University, GIP Cyceron, Caen, France

[4] Visual Cognition Lab, The Hebrew University of Jerusalem, Jerusalem, Israel

[5] Royal British Legion Centre for Blast Injury Studies, Department of Bioengineering, Imperial College London, London, UK

Correspondence to Dr Gregory Scott: gregory.scott99@imperial.ac.uk

Number of pages in manuscript = 44
Number of figures in manuscript = 11
Number of tables in manuscript = 3
Abstract word count = 227
Introduction word count = 641
Discussion word count = 1497

The work was supported by an Academy of Medical Sciences Starter Grant for Clinical Lecturers (awarded to NG) and by an equipment grant from the Department of Medicine, Imperial College London. E-JM is supported by the UK Dementia Research Institute Care Research and Technology Centre. GS is supported by NIHR. DJS is supported by the UK Dementia Research Institute Care Research and Technology Centre, an NIHR Professorship (NIHR-RP-011-048), the NIHR Clinical Research Facility and Biomedical Research Centre at Imperial College Healthcare NHS Trust & The Royal British Legion Centre for Blast Injury Studies.

The authors would like to thank all the participants who took part in this study. The authors also thank the staff at the Major Trauma Ward and the Neurosurgery, Emergency and Trauma Research Team, St Mary's Hospital, Imperial NHS Healthcare Trust, London, UK for their assistance in patient screening.
The authors declare no competing interests.

Abstract

Associative binding is key to normal memory function and is transiently disrupted during periods of post-traumatic amnesia (PTA) following traumatic brain injury (TBI). Electrophysiological abnormalities including low-frequency activity are common following TBI. Here, we investigate associative memory binding during PTA and test the hypothesis that misbinding is caused by pathological slowing of brain activity disrupting cortical communication. Thirty acute moderate-severe TBI patients (25 males; 5 females) and 26 healthy controls (20 males; 6 females) were tested with a precision working memory paradigm requiring the association of object and location information. Electrophysiological effects of TBI were assessed using resting-state EEG in a subsample of 17 patients and 21 controls. PTA patients showed abnormalities in working memory function and made significantly more misbinding errors than patients who were not in PTA and controls. The distribution of localisation responses was abnormally biased by the locations of non-target items for patients in PTA suggesting a specific impairment of object and location binding. Slow wave activity was increased following TBI. Increases in the delta-alpha ratio indicative of an increase in low-frequency power specifically correlated with binding impairment in working memory. Connectivity changes in TBI did not correlate with binding impairment. Working memory and electrophysiological abnormalities normalised at six-month follow-up. These results show that patients in PTA show high rates of misbinding that are associated with a pathological shift towards lower frequency oscillations.

Significance Statement

How do we remember what was where? The mechanism by which information e.g., object and location is integrated in working memory is a central question for cognitive neuroscience. Following significant head injury, many patients will experience a period of post-traumatic amnesia (PTA) during which this associative binding is disrupted. This may be due to electrophysiological changes in the brain. Using a precision working memory test and resting-state EEG we show that PTA patients demonstrate impaired binding ability, and this is associated with a shift towards slower frequency activity on EEG. Abnormal EEG connectivity was observed but was not specific to PTA or binding ability. These findings contribute to both our mechanistic understanding of working memory binding and PTA pathophysiology.

Introduction

Post-traumatic amnesia (PTA) is a transient state of cognitive impairment following traumatic brain injury (TBI), characterised by disorientation and mnemonic deficits. PTA is usually short-lived, but duration is highly variable and may persist throughout inpatient care (Marshman et al., 2013). PTA duration predicts TBI severity, with longer periods associated with poorer functional outcomes (Ponsford et al., 2015; Friedland and Swash, 2016). Reduced connectivity between parahippocampal gyrus and posterior cingulate cortex is associated with working memory impairments which resolve upon PTA emergence (De Simoni et al., 2016). This suggests that working memory impairments during PTA result from disruption to cortical communication between brain regions involved in encoding information held in working memory.

A range of memory impairments are present in PTA (Hennessy et al., 2021). In visual working memory, information about an object's identity and location must be encoded and bound together (Schneegans and Bays, 2018). Binding is a sensitive measure of working memory impairment in various disease states (Parra et al., 2010, 2015; Liang et al., 2016). A precision working memory paradigm allows recognition memory for object identification, free recall of spatial location and the source of errors to be independently quantified (Pertzov et al., 2012). This allows detailed investigation of working memory impairment in PTA which we use to investigate whether binding failures are associated with electrophysiological abnormalities that potentially disrupt cortical communication.

Neural oscillations are central to working memory function (Luo and Guan, 2018). Long-range theta phase synchronisation supports communication between prefrontal cortex and temporal

lobe during encoding, retrieval and working memory maintenance (Fell and Axmacher, 2011). Frontal theta phase also modulates temporal-parietal gamma amplitude in a process known as phase-amplitude coupling (PAC). Theta-gamma PAC is important in encoding, working memory and associative binding and is mechanistically supported by long-range theta synchronisation (Lega et al., 2016; Daume et al., 2017; Köster et al., 2018). Theta rhythms, and interactions with other frequencies, therefore have a primary role in associative memory that likely underpins memory processes at the large-scale network level (Jann et al., 2010; Yuan et al., 2012; Hacker et al., 2017). The precise synchronisation of neural oscillations necessary for working memory may be sensitive to disruption by large electrophysiological abnormalities that often occur transiently after head injury.

Increased low-frequency oscillations are seen in many disease states, including TBI (Modarres et al., 2017; Jafari et al., 2020). Increased slow-wave activity is associated with poorer neurological outcome, personality change and cognitive impairment following TBI (Huang et al., 2014; Robb Swan et al., 2015). Relative changes can be described using delta-alpha ratio (DAR) reflecting the difference in contribution between delta and alpha. Reducing DAR using transcranial electrical stimulation improves cognition after TBI (Ulam et al., 2015). Synchronisation disturbances are also present following TBI including decreased gamma connectivity (Wang et al., 2017), reduced connectivity across theta, alpha and beta associated with working memory impairment (Kumar et al., 2009; Bailey et al., 2017) and improved cognition with reduced delta connectivity (Castellanos et al., 2010). Cross-frequency coupling is also disrupted following TBI (Antonakakis et al., 2016). Taken together, this suggests that a shift to pathological low-frequency power after TBI may be mechanistically important for

working memory disturbance by disrupting the neural oscillations that support the maintenance of information in working memory.

Here for the first time, we investigate working memory binding in an acute cohort of moderate-severe TBI patients with and without PTA. Electrophysiological abnormalities are quantified using EEG. We test the following hypotheses: 1) PTA patients will show increased misbinding errors; 2) PTA will be associated with increased low-frequency oscillations; 3) binding impairment will correlate with increased low-frequency oscillations reflected in increased DAR; 4) PTA will be associated with abnormal long-range theta phase synchronisation and theta-gamma PAC; 5) Emergence from PTA will be associated with a reduction in misbinding and a normalisation of EEG measures.

Materials and Methods

Participant demographics and clinical details

Traumatic brain injury group

Thirty patients (25 males, five females, mean age 40.73, range 17-73 years) admitted with a recent history of TBI were recruited from the Major Trauma Ward, St Mary's Hospital, London, UK. All patients had moderate-severe injuries according to the Mayo Classification system for TBI severity (Malec et al., 2007). Injuries were secondary to road traffic accidents (40.0%), falls (33.3%), assault (20.0%) and sports injury (6.67%). Patients were included if they were between the ages of 16-80 and clinically stable. Exclusion criteria were as follows: premorbid psychiatric or neurological illness; history of other significant TBI; current or previous drug or alcohol abuse; pregnancy or breastfeeding; significant language or

visuospatial impairments. For the EEG part of the study, neurosurgical intervention (or other contraindication to scalp EEG) was also an exclusion criterion. Detailed clinical characteristics of all TBI patients are available in Extended Data Table 1-1.

Written informed consent was obtained for patients judged to have capacity according to the Declaration of Helsinki. Patients in PTA who were judged not to have capacity were deemed unable to give informed consent for participation in the study. In this case, written assent was obtained as well as informed written assent by a caregiver on the patient's behalf. Informed consent was gained retrospectively once patients emerged from PTA. No patients withdrew consent. The study was approved by the West London Research Ethics Committee (09/HO707/82).

Control group

26 healthy controls (20 males, 6 females, mean age 28.96, range 18-70 years) were recruited friends/relatives of TBI patients or through word of mouth. Participants had no history of psychiatric or neurological illness, previous TBI or alcohol or substance misuse. All participants gave written informed consent.

Protocol

At baseline, all participants underwent neuropsychological assessment, precision working memory task and resting-state EEG. Additionally, patients underwent PTA assessment according to the Westmead Post Traumatic Amnesia Scale (WPTAS; Shores et al., 1986). The WPTAS is a 12-item scale with seven items that assess orientation and five items that assess memory. Patients must score full marks (12/12) for three consecutive days before they are deemed to no longer be in PTA. PTA duration is calculated as the time between injury and the

first of these successful consecutive assessments. Patients were on average within 10 days of injury (range 1-32 days) and were divided into two groups (PTA+ and PTA-). PTA status was confirmed using clinical notes and WPTAS scores on the days surrounding the assessments. Patients were thus classified as PTA+ or PTA- according to standard clinical criteria as detailed above. Patients were invited to attend follow-up assessment within six months of hospital discharge, at which the baseline protocol was repeated. Controls were assessed at one timepoint.

Where possible, participants took part in all aspects of the study. However, due to the nature of recruitment within an acute clinical setting this was not always possible or appropriate. A subsample of 17 patients and 21 controls underwent resting-state EEG. Of these, there was one patient and one control who did not complete the precision working memory task.

Neuropsychological assessment

All participants completed a detailed neuropsychology assessment with a focus on episodic and working memory. Immediate and delayed verbal recall were assessed using The Logical Memory I and II subtests of the Wechsler Memory Scale, third edition (Wechsler, 1997). Immediate and delayed visuospatial memory were assessed using the Brief Visuospatial Memory Test-Revised (Benedict et al., 1996). Delayed recall elements of the neuropsychology tasks were administered 25 minutes after the initial assessment. A battery of computerised tests based on classical paradigms from the cognitive psychology literature was delivered on a tablet device using a custom-programmed application. Details of each task have been previously reported (Hampshire et al., 2012). In brief: Visuospatial Working Memory, based on a task from the non-human primate literature was used to assess visuospatial working memory(Inoue and Matsuzawa, 2007); Paired Associates, based on a paradigm commonly used to assess

memory impairments in aging clinical populations was used to assess object-location association memory (Gould et al., 2005); Spatial span, based on the Corsi Block Tapping Task was used to assess spatial short term memory capacity (Corsi, 1973); Self-Ordered Search was used to measure strategy during search behaviour, based on an existing task (Collins et al., 1998); Feature Match, based on the classical feature search task was used to measure attentional processing (Treisman and Gelade, 1980).

Statistical analysis of neuropsychological data

One-way ANOVAs were used to identify group effects at baseline. Post-hoc independent samples pairwise t-tests, using false discovery rate (FDR) multiple comparisons corrections were performed to determine which pairwise comparisons were driving any significant main effects. Linear mixed-effects models were used to assess longitudinal changes between baseline and follow-up in which group and time point were defined as fixed effects and subject was defined random intercepts included for each subject. Post-hoc paired samples t-tests were used to investigate any significant main effects or interactions. Unless otherwise stated all statistical analysis was performed using R (Version 1.3.1056).

Experimental task paradigm

Classic span tasks are sensitive to general impairments of working memory, but don't allow the binding of information to be specifically studied. Recently, precision working memory tasks have been developed that allow recognition memory for object identity and spatial location to be measured separately from the binding of this information e.g., providing separate tests of whether an object was remembered, and whether the spatial location of that object was remembered. Participants completed a precision recall working memory task (Figure 1A) based on Pertzov et al. (2012).

The stimuli consisted of 60 fractal images (Sprott, 1996). Fractals were used as complex visual objects that unlike images of everyday objects cannot be readily verbalised. A maximum width and height of 120 pixels was used. Stimuli were presented on an interactive touch-sensitive screen with a 1920 x 1080 pixel matrix (Dell Corp. Ltd). The experiment consisted of 80 trials (20 1 item; 60 2 item). Object location was determined by a Matlab script (MathWorks) with (x,y) coordinates randomly drawn from across the horizontal and vertical pixel dimensions of the screen, respectively, with the following exceptions: objects were never located within 600 pixels of each other within a single trial. They were positioned within a minimum distance of 200 pixels from the screen edge. The threshold for the distance at which the response matched the target (or distractor) was set to 200 pixels.

Task procedure

Each trial began with a central fixation point followed by the memory array consisting of 1 or 2 distinct fractals presented for 2 seconds. A blank screen was displayed for 2 seconds (maintenance period) after which the object identification stage began in which two fractals were displayed alongside one another in the centre of the screen. One fractal had been present in the memory array of that trial, the other was a foil item that was not present in the memory array. Participants were required to touch the item that they remembered from the memory array and then drag it to the remembered location. Localisation performance was only analysed in trials in which the object identity was correctly remembered.

Task analysis

Data from the precision working memory task were analysed using a thresholded approach in which a correct localisation was considered to be within 200 pixels of the target (or a

misbinding error within 200 pixels of the non-target) to calculate a proportion of misbinding errors. A novel, threshold-free approach to study the distribution of responses across a transformed space, defined by the relative locations of target versus non-target items was used to visualise the distribution of responses across trials (Figure 1B). In this transformed space the target position is located at the origin and the non-target at 1,0 (*x*,*y*). Therefore, responses deviating from the origin along the x-axis indicate a spatial bias by the non-target item location, as happens when the target identity is misbound with the non-target location. In contrast, responses deviating along the y-axis do not indicate a spatial bias by the non-target location but are in-keeping with imprecision in remembering the correct location, or with random error (Figure 1C). The responses in this transformed space are binned across ten uniformly spaced bins. This approach allows the influence of the non-target on the remembered location to be visualised without dichotomising responses based on arbitrarily defined thresholds. The design of this paradigm thus allowed us to measure the distinct processes of object-location associative memory independently to quantify the types of error made, i.e., failure to remember the location or failure to bind.

EEG data acquisition

EEG data were acquired using a 32-channel active electrode standard actiCAP positioned with Cz at the midline with electrodes grounded to FPz and referenced to Fz. Signals were amplified using the actiCHamp system and data recorded using the BrainVision Recorder software (Brain Products) at a sampling rate of 1000 Hz.

EEG pre-processing

Raw EEG data were exported from BrainVision into Matlab via EEGLAB. Data were pre-processed, cleaned and quality assessed using the Harvard Automated Processing Pipeline for EEG (HAPPE), an automated pre-processing pipeline specifically developed for high artefact data as would be expected in acute TBI patients. HAPPE has been shown to be superior in optimising signal to noise ratio compared to manual editing in clinical data (Gabard-Durnam et al., 2018). The following pre-processing steps were taken using the HAPPE pipeline: Data were high-pass filtered at 1Hz, low-pass filtered at 100Hz and band-pass filtered at 1- 249Hz as recommended for HAPPE processing. Electrical line noise at 50Hz was removed using the CleanLine multi-taper approach (Mullen T, 2012). Bad channels (i.e., those with poor signal quality) were rejected using joint probability evaluation and those exceeding 3 SD from the mean were excluded from further analyses (to be later interpolated). Wavelet-enhanced independent component analysis (wICA) was performed to correct for EEG artefact while retaining the whole dataset to improve ICA decomposition. ICA was performed on the corrected data and components were rejected using the multiple artifact rejection algorithm (MARA) (Winkler et al., 2011). HAPPE rejects components with artifact probabilities > 0.5. Data were segmented into 5-second segments and subjected to amplitude-based (+/- 40μV) and joint-probability (< 3 SDs relative to the activity of other segments) rejection to remove

segments with remaining artefact. Previously rejected channels were repopulated using spherical interpolation. Data were re-referenced to average.

EEG analysis

Channels were grouped into four regions: frontal (‘*Fp1’, ‘Fp2’, ‘F3’, ‘F4’, ‘F7’, ‘F8’*), temporal *(‘T7’, ‘T8’, ‘TP9’, ‘TP10’, ‘FT9’, ‘FT10’),* parietal (‘*Pz’, ‘P3’, ‘P4’, ‘P7’, ‘P8’*), occipital (‘*O1’, ‘O2’, ‘Oz’)*. Frequency bands were defined as follows: delta (0-4Hz); theta (4-8Hz); alpha (8-13Hz); beta (13-30Hz) and gamma (30-40Hz).

Normalised power

Power in each channel was calculated for each frequency band using multitaper frequency transformation normalised to total power across all five bands. Global power was calculated by averaging across all channels.

Statistical comparison of global normalised power was conducted using one-way independent measures ANOVA followed by post-hoc *t*-tests. All *p*-values were corrected using FDR method for multiple comparisons. Group-level statistical analysis of normalised power was also performed using a cluster-based permutation approach in the frequency/channel domain on the whole montage (Maris and Oostenveld, 2007). Power was compared between groups at each channel using two-sided independent samples t-tests and results clustered according to spatial adjacency at $P<0.05$ using the maximum size criterion. Permutation distributions were generated using the Monte-Carlo method and 5000 random iterations, and corrected *p*-values were then obtained through comparison of observed data to the random distributions. Follow-up data was assessed as above. No cluster-based permutation analysis was performed on follow-up data.

Phase synchronisation

Phase synchronisation was quantified using the debiased weighed phase lag index (dwPLI) a measure of phase based functional connectivity. Phase lag index (PLI) calculates to what extent the phase of one signal is consistently lagging or leading relative to another signal, irrespective of the magnitude of the phase leads and lags (Stam et al., 2007). The weighted PLI is weighted by the imaginary component of the cross-spectrum to overcome issues with spuriously related connectivity which can arise due to volume conduction (Vinck et al., 2011). A further debiasing term to correct for inflation due to small sample size was additionally implemented within the ft_connectivity_wpli.m function in FieldTrip (Oostenveld et al., 2011). dwPLI is calculated across all frequencies within the band of interest for each channel pair.

To statistically compare connectivity at the group level we constructed 31x31 whole brain channel-wise connectivity matrices for each subject by averaging dwPLI values for each channel pair across the frequency band. The network-based statistic (NBS) implemented in MATLAB was used to compare connectivity across groups using an independent samples *t*-test design (Zalesky et al., 2010). The NBS is a non-parametric statistical method in which values at every node are tested against the null-hypothesis and those surviving the primary threshold are entered for Monte-Carlo simulation permutation testing at every channel pair. The primary threshold was set to z=3.1 and 10,000 random permutations were conducted with a threshold of P<0.05.

Phase-amplitude coupling

To quantify the intensity of PAC between theta phase and gamma amplitude we computed the modulation index (MI; Tort et al., 2010). We estimated the phase of frequencies between 4-8 Hz (in steps of 1 Hz) in the frontal channel group and the amplitudes of frequencies between

30-40 Hz (in steps of 2 Hz) in parietal and temporal channel groups individually. The MI was calculated separately for each electrode within the respective channel groups.

To test for group differences in PAC, MI values were averaged across frontal-parietal and separately frontal-temporal channel groups for each participant and compared using independent samples Welch *t*-tests. In patients who returned for follow-up, within-subjects *t*-tests were used to assess differences in the dwPLI and MI across time.

Relationship between EEG and behavioural measures

We assessed the relationship between EEG measures and clinical information such as duration of PTA or behavioural performance using Pearson correlations. To assess whether the relationship between variables differed between groups, the correlation coefficients were compared using Fisher's *z* statistic implemented in the '*cocor'* package in R.

Data availability

The data that support the findings of this study are available from the authors upon reasonable request.

Results

Clinical demographics

Thirty moderate-severe TBI patients were recruited during their in-patient stay (age range 17-73 years; Table 1). Seventeen patients were in PTA at the time of enrolment (PTA+, mean WPTAS 9.18, *SD*=1.38). Thirteen patients were not in PTA (PTA-, WPTAS 12 for all). The PTA+ group had a longer PTA duration and longer hospital admission, but groups did not differ in time since injury (Table 1). PTA+ and PTA- groups were well matched for age (*P*=0.95) and gender (Table 1).

Twenty-six control participants were recruited (age range 18–70 years; Table 1). ANOVA showed an effect of age across the groups driven by controls being younger than both PTA+ and PTA- patients (Table 1). Additionally, there were group differences in years of education due to the PTA+ group having fewer years of education than controls and the PTA-group (Table 1).

Table 1. Clinical demographics for all participants

	Controls (n=26)		PTA+ (n=17)		PTA- (n=13)		Statistic	*P*	Post-hoc differences
	Mean	SD	Mean	SD	Mean	SD			
Days since injury			11.00	8.87	8.69	8.07	t = -0.74	0.464	
PTA duration			14.94	11.28	4.58	8.14	t = 2.87	0.008**	
Admission duration			16.76	11.39	8.23	7.83	t = 2.43	0.021*	
Age	28.96	11.85	40.88	15.18	40.54	16.31	F = 4.92	0.011*	PTA+>CON *P = 0.026** PTA->CON *P = 0.028**
Years of education	16.42	2.58	13.12	1.90	16.38	2.69	F = 10.93	0.0001***	PTA+<CON *P = 0.0002**** PTA->PTA+ *P = 0.0009****
Sex (M:F)	20:6		15:2		10:3		Fisher's Exact	0.681	

*P < 0.05; **P < 0.01; ***P < 0.001; CON = Controls; M = male; F = female; PTA+ >CON = patients in PTA showed increased mean compared to healthy controls; PTA- > CON = patients not in PTA showed increased mean compared to healthy controls; PTA+<CON = patients in PTA showed reduced mean compared to healthy PTA- >PTA+ = patients in PTA showed increased mean compared to patients not in PTA. Detailed clinical characteristics of each patient are available in Extended Table 1-1.

Neuropsychological performance

TBI patients generally had significant cognitive abnormalities (Figure 2; Table 2), with impairments in the following relative to controls: immediate and delayed verbal memory, immediate and delayed visuospatial memory, associative working memory, spatial short-term memory, search strategy and attentional processing. There were no group differences in retention rates between immediate and delayed recall for either verbal memory or visuospatial memory.

Patients in PTA also showed impairments compared to both PTA- patients and controls in the following: immediate verbal recall, delayed visuospatial memory recall, associative working memory and search strategy. PTA patients also showed impairments compared to controls in delayed verbal memory recall, immediate visuospatial memory recall, visuospatial working memory, short term spatial memory and attentional processing (Figure 2; Table 2).

Table 2. Neuropsychology at baseline

Cognitive Domain	Neuropsychological Test	CON Mean (± SD)	PTA+ Mean (± SD)	PTA- Mean (± SD)	ANOVA Group Effect F	p	Post-hoc group differences (FDR corrected)
Verbal Memory	Logical Memory Immediate Recall	45.33 (9.76)	24.57 (13.74)	36.64 (8.94)	11.20	0.0002	PTA+ < CON (p=0.0001)*** PTA+ < PTA- (p=0.0176)*
	Logical Memory Delayed Recall	29.17 (8.12)	13.14 (10.69)	21.36 (8.82)	9.46	0.0005	PTA+ < CON (p=0.0004)***
	Logical Memory Retention	87.57 (11.93)	65.79 (43.34)	78.27 (19.06)	1.786	0.183	
Visuospatial Memory	BVMT Immediate Recall	28.92 (7.05)	16.80 (9.81)	23.00 (7.16)	7.572	0.002	PTA+ < CON (p=0.0012)**
	BVMT Delayed Recall	10.46 (2.44)	5.93 (4.18)	8.83 (2.82)	6.66	0.003	PTA+ < CON (p=0.0029)** PTA+ < PTA- (p=0.0454)*
	BVMT Retention	0.92 (0.12)	0.72 (0.35)	0.97 (0.37)	2.40	0.1058	
	Visuospatial Working Memory	7.65 (0.93)	6.20 (1.47)	6.62 (1.76)	5.26	0.0089	PTA+ < CON (p=0.0098)**
Associative Working Memory	Paired Associates Learning	5.05 (1.19)	3.40 (0.99)	4.62 (1.04)	10.09	0.0002	PTA+ < CON (p=0.00018)*** PTA+ < PTA- (p=0.00779)**
Spatial Short Term Memory	Spatial span	6.05 (1.47)	4.43 (1.70)	5.31 (1.44)	4.63	0.0150	PTA+ < CON (p=0.0120)*
Search Strategy	Self-ordered search	7.75 (1.33)	5.07 (1.58)	7.38 (1.61)	15.24	<0.0001	PTA+ < CON (p<0.0001)*** PTA+ < PTA- (p=0.00025)***
Attentional Processing	Feature Match	150.45 (33.41)	78.87 (33.68)	104.85 (35.51)	19.48	<0.0001	PTA+ < CON (p<0.0001)*** PTA- < CON (p=0.00082)***

* P < 0.05; ** P < 0.01; *** P < 0.001; CON = Controls; PTA+ < CON = patients in PTA showed reduced mean compared to healthy controls; PTA- < CON = patients not in PTA showed reduced mean compared to healthy controls; PTA+ < PTA- = patients in PTA showed reduced mean compared to patients not in PTA

Impaired working memory binding in post-traumatic amnesia

A precision working memory task was used to assess the binding of object and location information in working memory. All three groups identified the target with >90% accuracy, indicating that subjects understood the task regardless of whether they were in PTA (Figure 3A). As expected, accuracy decreased as working memory load increased, with two item trials less accurate than one item trials ($F(1,51) = 55.32$, $P<0.001$). There was also a group effect of object identification ($F(2,51)=9.98$, $P<0.001$): PTA+ patients showed more errors in identifying targets than PTA- patients ($t(105)=3.49$, $P=0.001$) and controls ($t(105)=-5.46$, $P<0.001$). A group by load (1 or 2 item trial) interaction was present of borderline significance ($F(2,51)=2.89$, $P=0.065$).

Similar results were observed when considering the spatial accuracy of target placement (Figure 3B). A group by load interaction was present ($F(2,51)=7.32$, $P=0.002$), due to PTA+ patients showing less accurate placements compared to PTA- patients ($t(105)=4.10$, $P<0.001$) and controls ($t(105) =-6.31$, $P<0.001$) in 2 item trials. Figure 3C shows the distribution of responses in relation to the target and non-target items in the normalised space.

Next, we quantified the numbers of misbinding errors, defined as a response being placed within 200 pixels of the non-target location. There was a group effect on misbinding errors ($F(2,51)=25.62$, $P<0.001$), the result of PTA+ patients making significantly more misbinding errors than PTA- ($t(51) =-5.60$, $P<0.001$) and controls ($t(51)=6.65$, $P<0.001$; Figure 3D). There was no relationship between years of education and misbinding errors in TBI patients ($R=-0.43$, $P=0.10$).

Impaired binding ability is transient and specific to a period of PTA

Eighteen patients returned for follow-up (average 182 days post-baseline). Cognitive function generally improved at follow-up (Figure 4; Table 3), and memory binding in PTA+ patients normalised (Figure 3E). There was a group by visit interaction ($F(1,15)$=20.99, P<0.001). This was driven by a reduction in misbinding errors in PTA+ patients between visits but no longitudinal change in PTA- patients (Figure 3F; PTA+ v1 > PTA+ v2 (t(7)=4.60, P=0.0025); PTA – v1 > PTA- v2 (t(8)=-0.180, P=0.862)).

Table 3. Neuropsychology at follow-up

				Mixed Effects Model					
Cognitive Domain	**Neuropsychological Test**	**PTA+ Mean (± SD)**	**PTA- Mean (± SD)**	**Group**		**Timepoint**		**Group x Timepoint**	
				F	**p**	**F**	**p**	**F**	**p**
Verbal Memory	Logical Memory Immediate Recall	32.86 (9.41)	39.89 (4.94)	3.65	0.0785	5.32	0.0415*	0.08	0.7786
	Logical Memory Delayed Recall	20.43 (8.58)	27.22 (3.80)	3.79	0.0734	23.52	0.0005***	0.39	0.5474
	Logical Memory Retention	84.71 (25.65)	93.65 (10.81)	0.11	0.7510	5.14	0.0445*	1.88	0.1975
Visuospatial Memory	BVMT Immediate Recall	23.71 (8.38)	27.56 (5.32)	2.13	0.168	5.16	0.0424*	0.11	0.7487
	BVMT Delayed Recall	8.14 (4.22)	11.11 (0.93)	5.30	0.0385 *	1.729	0.2130	0.05	0.8340
	BVMT Retention	0.89 (0.43)	0.97 (0.04)	2.04	0.1770	0.011	0.9190	0.75	0.4020
	Visuospatial Working Memory	7.00 (1.51)	7.75 (1.04)	2.42	0.144	1.53	0.2380	0.01	0.9380
Associative Working Memory	Paired Associates Learning	4.00 (0.76)	4.62 (1.06)	8.02	0.0142 *	0.126	0.7280	0.14	0.710
Spatial Short Term Memory Capacity	Spatial span	5.62 (0.74)	5.88 (1.36)	0.70	0.4190	2.49	0.1390	0.18	0.6800
Search Strategy	Self-ordered search	7.25 (1.98)	8.12 (1.55)	6.15	0.0277 *	6.54	0.0238*	1.61	0.2263
Attentional Processing	Feature Match	110.25 (28.31)	128.12 (27.66)	1.57	0.2330	5.40	0.0370*	0.29	0.601

Patients in post-traumatic amnesia show increased low-frequency power

Resting EEG showed changes in power across a range of frequency bands in patients with PTA (delta: $F(2,35)=5.97$, $P=0.009$; alpha: $F(2,35)=9.05$, $P=0.003$; gamma: $F(2,35)=5.08$, $P=0.014$; false-discovery rate corrected; Figure 5A). In the delta band, these effects were driven by PTA+ patients exhibiting increased power compared to controls (PTA+ > CON: $t(35)=3.43$, $P=0.005$) and a trend towards an increase compared to PTA- (PTA+ > PTA-: $t(35)=-2.16$, $P=0.057$). In the alpha band, PTA+ showed reduced power compared to controls (PTA+ < CON: $t(35)=-4.25$, $P<0.001$) and a trend towards a decrease compared to PTA- (PTA+ < PTA-: $t(35)= 2.09$, $P=0.065$). PTA+ patients also showed reductions in beta power (PTA+ < CON: $t(35)=-3.01$, $P=0.014$; PTA- < CON: $t(35)=-2.66$, $P=0.018$). In the gamma band, the PTA- group showed reduced power compared to controls (PTA- < CON: $t(35)=-2.97$, $P=0.016$), with no differences in the PTA+ group.

Visual inspection of topoplots displaying group means (Figure 5C) indicated abnormal patterns of power across multiple frequency bands in both TBI groups. Absolute differences between groups are displayed as raw contrasts in Figure 6A. Cluster-based statistics were used to quantify the differences between groups (Figure 6B). In the delta band, direct comparison between patient groups and controls showed increased power for both PTA+ ($P=0.002$) and PTA- patients (P=0.002) in frontal, parietal, and temporal channels, with PTA+ showing a more widespread cluster extending into occipital channels. There were no significant clusters arising from a contrast between PTA+ and PTA- patients. Conversely in the alpha band, PTA+ showed reduced (P=0.001) occipital and right parietal power compared to controls, and widespread reductions compared to PTA- in frontal, temporal, and parietal channels (P=0.007). There were no significant differences between PTA- and controls. In the theta band, PTA+

patients showed reduced theta power (P=0.049) compared to PTA- in a right parietal-occipital cluster of channels, while PTA- showed increased theta power (P=0.003) compared to controls in temporal and parietal channels. Changes in the beta band were of a similar pattern to theta. The PTA- group showed increased power in temporal and parietal channels compared to controls (P=0.023) and increased parietal power compared to PTA+ (P=0.004). There were no clusters found between any of the groups in the gamma frequency band.

EEG abnormalities in the PTA+ group were transient, and power had normalised at follow-up (Figure 7A). There was a significant effect of visit in delta and alpha (delta: $F(1,8) = 13.65$, P=0.006; alpha: $F(1,8)=8.37$, P=0.020). This was the result of increases in alpha and decreases in delta in the PTA+ group between baseline and follow-up (alpha: PTA+v1 < PTA+v2 ($t(4)=-4.0726$, P=0.030); delta: PTA+v1 > PTA+v2 ($t(4)=4.1234$, P=0.029)). There was also a significant group by time interaction in beta and gamma but no longitudinal effects were observed in theta (beta: $F(1,8)=13.23$, P=0.007; gamma: $F(1,8)=6.30$, P=0.036). Figure 7C depicts the spatial distribution in channel space of the change across time (follow-up minus baseline) for each frequency band for PTA+ and PTA- patients.

EEG differences between PTA+ and PTA- were particularly marked in delta and alpha bands, so the delta/alpha ratio (DAR) was calculated. DAR has been used as a sensitive marker of cerebral dysfunction (Claassen et al., 2004; Schleiger et al., 2014; Finnigan et al., 2016). Group differences in global DAR were present (Figure 5B; $F(2,35)=9.12$, P<0.001), the result of significantly higher in PTA+ compared to both PTA- ($t(35)=-2.51$, P=0.025) and controls ($t(35)=4.26$, P<0.001). Abnormalities in DAR normalised at follow-up, as demonstrated by a significant group by time interaction ($F(1,8)=5.48$, P=0.047), the result of a reduction in DAR

in PTA+ with no change in PTA- group (PTA+v1 > PTA+v2: $t(4)=3.008$, $P=0.040$; Figure 7B).

Individual case studies

To better describe the transient binding impairment and how this might relate to the transient shift towards slow wave power, we considered these changes at the single patient level. Figure 8 illustrates four individual case studies to highlight that the EEG changes reported here are more sensitive to abnormalities occurring during a period of PTA than conventional routine clinical imaging. Case studies one to three show TBI patients during a period of PTA at baseline and at follow-up once they were no longer in PTA. Case study four shows a TBI patient who was not in PTA. We include these case studies to highlight that the group-level findings are also observable in individual patients and therefore have the potential to be clinically meaningful.

Case study one is a 45-year-old male with a moderate-severe TBI acquired through a fall from standing. Clinical imaging reported presence of subdural haemorrhage (SDH), subarachnoid haemorrhage (SAH), bi-frontal contusions and midline shift. On the day of assessment (day eight post-injury, WPTAS score 8) he was clinically deemed to be in PTA and had a total PTA duration of 12 days. At baseline he showed a bias towards the non-target on the precision working memory task with 34% rate of misbinding errors. He showed a dramatic improvement at follow-up to 12.7% misbinding errors. At baseline he had a global DAR of 6.46 which reduced to 0.99 at follow-up.

Case study two is a 26-year-old male with a moderate-severe TBI acquired through a cycling collision. There was no intracranial haemorrhage or space-occupying lesions on the initial clinical imaging. Further imaging with MRI revealed evidence of diffuse axonal injury (DAI). He was assessed on day 24 post-injury, scoring 7 on the WPTAS and thus still in a period of PTA. He had a total PTA duration of 38 days. Working memory binding performance at baseline was poor with misbinding of 22.6% which reduced to 5.6% at follow-up. At baseline his global DAR was 6.52 and reduced to 0.82 at follow-up.

Case study three, a 67-year-old male, acquired a moderate-severe TBI acquired while cycling. He had a total PTA duration of 28 days. Clinical imaging showed a left SDH, left temporal contusions, (probable) right extradural haemorrhage (EDH), skull base fractures and pneumocephalus. On assessment he was clinically deemed to be in PTA (WPTAS score 8; day 5 post-injury). At baseline he made 20% misbinding errors which improved to 5.6% at follow-up. His global DAR was 4.21 at baseline and reduced to 0.75 at follow-up.

Case study four is a 33-year-old male with a moderate-severe TBI acquired through a road accident as a pedestrian. Clinical imaging reported left-sided extra-axial haematoma with associated comminuted fracture involving the left frontal bone. Evidence of DAI was present on MRI. He had a PTA duration of 0 days and was thus not in PTA at the time of assessment (WPTAS score 12; day 5 post-injury). At baseline he demonstrated extremely low rates of misbinding (1.7%) which increased slightly at follow-up to 3.4%. At baseline he had a global DAR of 2.04 which decreased to 0.48 at follow-up.

Power abnormalities in acute TBI are associated with working memory performance

To quantify the relationship between EEG measures and working memory performance following TBI, we grouped PTA+ and PTA- patients to examine the relationship between a shift towards low-frequency power and cognitive performance (Figure 9). We first assessed delta and alpha individually in order to understand what the relative contributions of each of these frequencies were to any relationships between DAR and cognition.

Global delta power was associated with working memory performance in TBI patients but not controls (Figure 9A; Misbinding errors (TBI: R=0.52, P=0.038; Controls: R=-0.07, P=0.780); Paired associates learning (TBI: R=-0.56, P=0.018; Controls: R=0.24, P=0.38)). The correlation coefficients differed significantly between patients and controls for the relationship between global delta and performance on the paired associates learning task (z = 2.51, P=0.01) but did not differ for the relationship between global delta and misbinding errors (z = -1.75, P = 0.08).

Global alpha power was positively associated with performance on the paired associates learning task in TBI patients but showed a negative relationship to performance in controls (TBI: R=0.74, P<0.001; Controls: R=-0.58, P=0.025). The relationship between global alpha and performance on the PAL was significantly different between patients and controls (z = -4.27, P < 0.001). Global alpha showed a trend towards a relationship with misbinding errors in patients but showed no relationship in controls (Figure 9B; TBI: R=-0.49, P=0.06; Controls: R=0.15, P =0.52). There was a trend towards a difference in the correlation coefficients between patients and controls (z = 1.87, P= 0.06).

The global DAR significantly correlated with working memory performance in TBI patients but not healthy controls (Figure 9C; Misbinding errors (TBI: R=0.58, P=0.02; Controls: R=-0.23, P=0.33); Paired Associates Learning (TBI: R=-0.67, P=0.01; Controls: R=0.44, P=0.10)). The relationship between DAR and working memory performance differed significant between TBI patients and controls (Misbinding errors (Fisher's z = -2.45, P=0.01); Paired associates learning (Fisher's z = 3.21, P=0.001)).

Attentional processing was not associated with power in either delta or alpha frequency bands nor the DAR in either TBI patients or controls (global delta: TBI (R=-0.15, P=0.56); Controls(R=0.11, P=0.71); global alpha: TBI(R=0.057, P=0.83); Controls(R=0.22, P=0.42); DAR: TBI(R=-0.21, P=0.42); Controls(R=-0.039, P=0.89). The total duration of PTA, a proxy of injury severity, was not associated with power in either delta or alpha frequency bands nor in the DAR (global delta (R=0.23, P=0.39); global alpha (R=-0.27, P=0.32); DAR(R=0.46, P=0.08)).

The degree to which DAR was increased at baseline did not predict misbinding errors at follow-up in TBI patients (R=0.31, P=0.38). Rather, there was a relationship between normalisation of EEG measures and resolution of working memory impairment across time. When looking at changes between baseline and follow-up in TBI patients, there was a strong positive correlation between change in global DAR and change in misbinding errors (follow-up minus baseline; R=0.87, P=0.001).

TBI patients demonstrate theta hyperconnectivity and alpha hypoconnectivity

One mechanism through which a shift towards lower frequency power could be disrupting cortical communication is through altered connectivity across large scale networks. In order to test connectivity within the delta, theta, and alpha bands., phase synchronisation between electrodes was quantified using the dwPLI. Whole brain connectivity matrices were constructed on a channel-wise basis for controls and patients in each band separately (Figure 10A). Network based statistics revealed that patients show theta hyperconnectivity compared to controls across one robust network consisting of 19 edges and 15 nodes (P=0.005; Figure 10B). Connectivity within the theta network was not related to binding ability in TBI patients or Controls (TBI: R=0.19, P=0.49; Controls: R=0.09, P=0.70; Figure 10D). There was no difference in the mean connectivity within the theta network between PTA+ and PTA- patients (t(12.36)=0.66, P=0.52). There was a significant relationship between the mean dwPLI across the theta network and the total duration of PTA (R=0.57, P=0.016; Figure 10D).

In the alpha band there was a single robust network of hypoconnectivity in TBI patients compared to controls consisting of 6 edges and 6 nodes (P=0.020; Figure 10C). Connectivity within the alpha network was not related to binding ability in TBI patients or Controls (TBI: R=-0.23, P=0.39; Controls: R=-0.08, P=0.72; Figure 10F). There was no difference in the mean connectivity within the alpha network between PTA+ and PTA- patients (t(11.98)=0.38, P=0.71). The mean dwPLI in the alpha network did not show a relationship with PTA duration (R=-0.08, P=0.760; Figure 10F). At follow-up, whole-brain connectivity in the delta and theta bands decreased and increased in the alpha band (Figure 10A) and there was a general trend towards decreases in connectivity across the theta network and increases in connectivity across

the alpha network, though these were not statistically significant (theta: Figure 10E, $t(9)=1.81$, $P=0.103$; alpha: Figure 10G, $t(9)=-1.90$, $P=0.09$).

Mean connectivity within the alpha network showed a negative correlation to the DAR in controls (R=-0.48, P=0.028) but not in patients (R=-0.13, P=0.62). There was no relationship in either group between connectivity in the theta network and DAR (Patients: R=0.24, P=0.36; Controls: R=-0.41, P=0.067).

Theta-gamma cross-frequency coupling is not altered in acute TBI

Phase-amplitude coupling, specifically frontal theta phase to parietal and temporal gamma amplitude, was quantified using the MI. Contrary to our hypothesis, patients did not show increased phase-amplitude coupling for either frontal to parietal ($t(35.97)=-1.413$, $P=0.1662$) or frontal-temporal ($t(34.42)=-0.634$, $P=0.5303$) modulation (Figure 11A). There were no significant longitudinal changes in patients returning for follow-up in the mean modulation index for either frontal-parietal ($t(9)=1.567$, $P=0.1516$) or frontal-temporal ($t(9)=0.276$, $P=0.7891$) channels (Figure 11B). Separating the groups by PTA status did not produce an effect of group: there was no significant group effect on frontal-parietal theta-gamma PAC ($F(2,35)=1.83$, $P=0.175$) or frontal-temporal theta-gamma PAC (F(2,35)=2.46, P=0.100) when comparing PTA+, PTA- and healthy controls.

Discussion

Post-traumatic amnesia (PTA) is a common consequence of TBI characterised by profound but transient cognitive disturbances. Here, we show that PTA is associated with marked impairment in binding of information in working memory that resolves upon emergence from PTA. This behavioural abnormality is associated with a shift to low-frequency oscillations on EEG, quantified by increased delta-alpha ratio of EEG power (DAR), which is specifically seen in PTA and not TBI patients without PTA. Increased DAR correlated with misbinding failures, potentially indicating a causal role in the disruption of working memory function. Connectivity is non-specifically increased in the theta and decreased in the alpha following TBI. The results suggest that abnormal low-frequency oscillations, seen in many disease states, may disrupt the precise synchronisation of neural oscillations necessary for working memory function.

We used a precision spatial working memory task to assess binding of object-location information. Participants were required to accurately encode both the identity of an object and its spatial location. Separate identification and location phases probed identity and spatial information. Importantly, PTA patients had an accurate recognition memory for object identity in most trials. However, there were high levels of misbinding i.e., the correct object was chosen but moved to the incorrect location. This error was not random: PTA patients systematically chose the location of the non-target object from a free-recall space indicating that both spatial information and object identity had been independently encoded, but that the binding of this information was impaired.

Assessing misbinding relies on an arbitrarily defined threshold to decide whether a response is within the boundaries of a specific location and does not fully describe the response distribution across trials. It is informative to display responses in a transformed space as this can illustrate the presence of misbinding errors and the absence of random responses. We show clear clusters around target and non-target items demonstrating that spatial errors in PTA are non-random. This shows subjects are engaged, encode object identity and location but show binding impairments. This approach is also informative when applied to individual cases. The case studies highlight that transient increases in DAR and misbinding observed at the group level in PTA+ patients may also be informative at the single-subject level. A precision working memory task of this type could therefore be used to assess PTA, with misbinding measures offering a sensitive measure of how a PTA state changes over time.

While a key strength of the task design is the precision aspect of the spatial response, it is also possible that misbinding likelihood may be influenced by the proximity between the target and non-target items e.g., when positioned closer, a misbinding error may become more likely. To mitigate this risk, we kept a minimum distance of 600 pixels between target and non-target items. There was no correlation between a subject's misbinding rate and the mean distance between target and non-target ($R=0.0352$, $P=0.82$). Furthermore, there was no difference in the mean distance between target and non-target across groups ($F(2,24)=0.05$, $P=0.96$). Hence, the group level results we present could not be explained by any differences in proximity between target and non-target items.

Our PTA patients have widespread cognitive deficits compared to healthy controls. Some of these are produced by having an acute TBI, and are not specific to a period of PTA. Other

cognitive deficits are more pronounced in PTA+ compared to PTA-. Tasks requiring working memory integration, such as paired associates learning and object-search strategy, demonstrated differences between patient groups but those without the binding component (e.g., spatial-span) were less discriminatory. PTA+ also showed impaired attentional processing which may underpin some of their mnemonic deficits, though this was not related to misbinding (R=0.09, P=0.75). Attentional deficits would have made 'random' responses in their precision recall of location more likely but instead these were clustered around target and non-target locations. It is not therefore the case that PTA+ are globally more impaired than PTA- but rather there are transient and specific deficits, including binding ability, associated with PTA.

Resting-state EEG was used to identify electrophysiological abnormalities in acute TBI patients. In TBI, increased lower frequency power has previously been associated with long-term neuropsychological and functional outcomes (Leon-Carrion et al., 2009; Robb Swan et al., 2015). EEG slowing is often viewed as a nonspecific sign of cerebral dysfunction. We show that PTA patients show decreased alpha power, increased delta power and significantly higher DAR than TBI patients without PTA and controls. This abnormality correlated with misbinding and normalised at follow-up. Increased DAR may therefore be a sensitive electrophysiological marker of PTA that is closely related to the key cognitive impairments seen in this state.

Low-frequency oscillations are observed in other disease states (Howells et al., 2018; Cassidy et al., 2020; Jafari et al., 2020). Alzheimer's Disease patients show impaired binding (Della Sala et al., 2012) and a shift towards increased low-frequency oscillations characterised by delta synchronisation and alpha de-synchronisation (Benwell et al., 2020). Additionally,

increased low-frequency oscillations are associated with reduced awareness (Howells et al., 2018). We previously used voltage-imaging in rodents to show that anaesthesia is associated with low-frequency hypersynchrony and reduced cortical communication (Scott et al., 2014; Fagerholm et al., 2016). Increased low-frequency oscillations are therefore common to states of dementia, disordered consciousness, and PTA, and may provide a common electrophysiological mechanism by which the cortical dynamics necessary for higher cognitive functions, including working memory and awareness, are disturbed. PTA patients provide a unique way to study transient changes in the relationship between electrophysiological abnormalities and working memory binding. Here, we show that DAR normalises in conjunction with emergence from PTA and normalisation of working memory binding impairments. Taken together, our results suggest that the presence of increased low-frequency oscillations may disrupt electrophysiological interactions necessary for successful integration of object-location memory, and this mechanism may be relevant across a range of disease states. This study is observational and future interventional work such as animal modelling or brain stimulation studies would be required to establish a causal relationship between a shift towards more dominant lower frequencies and working memory failures.

To investigate how low-frequency oscillations might disrupt working memory, we explored the effect of TBI on cortical connectivity. Co-ordinated activity across the brain is important for communication. We calculated the phase-lag index (dwPLI) to quantify channel-wise correlations. Acute TBI patients showed theta hyperconnectivity and alpha hypoconnectivity, but these changes were not specific to PTA. Additionally, although theta connectivity between frontal and temporal-parietal regions has been shown to increase with working memory load and executive control (Fell and Axmacher, 2011), it did not correlate with binding performance

following TBI. However, theta connectivity increased with PTA duration, suggesting it might relate to injury severity (McMillan, 2015). We additionally explored phase-amplitude coupling in the theta/gamma bands, as this is associated with working memory binding (Daume et al., 2017; Köster et al., 2018). This was not abnormal following TBI and did not relate to binding performance. It is possible that we were simply not statistically powered to detect an effect. An alternative explanation for this is that changes in phase-amplitude coupling might only be seen during working memory performance. As we investigated resting-state EEG, we cannot explore the relationship between neural oscillatory dynamics and distinct working memory stages. Future work could usefully explore the relationship between EEG abnormalities and working memory impairment during event-related analyses of task performance.

Our patients were heterogenous in terms of TBI pathophysiology. The pattern of TBI seen on neuroimaging varied but did not explain the presence or absence of PTA. Importantly all patients in both PTA+ and PTA- groups sustained a moderate-severe TBI and it is not the case that the PTA+ group were merely more severely injured. Nevertheless, future work in a larger sample might investigate the relationship between distinct types of brain injury and the EEG/behavioural abnormalities we have observed. Additionally, the PTA group were older than controls. This is unlikely to explain our results. During healthy ageing there is a linear decrease of slow frequency resting-state activity (Vlahou et al., 2014). This suggests that if age were influencing the results, PTA+ patients would be expected to show lower delta power than controls. In fact, the opposite was observed, and PTA+ showed significantly greater delta power. A difference in age between the groups should therefore not alter the interpretation of a shift towards lower frequency oscillations during PTA. Finally, our PTA+ patients had fewer education years than PTA- patients. However, there was no relationship between education

years and proportion of misbinding errors in TBI patients, and we do not therefore think that this difference can explain the behavioural results observed.

In summary, acute TBI patients experiencing PTA show a marked impairment of associative working memory. We quantified this using misbinding errors and showed how this relates to electrophysiological changes on EEG. Our results demonstrate a clear relationship between a shift to pathological oscillatory slowing and transient working memory impairment in PTA, which is informative in understanding the profound but transient effects of TBI on higher cognitive functions.

References

Alekseichuk I, Turi Z, Amador de Lara G, Antal A, Paulus W, Amador de Lara G, Antal A, Paulus W (2016) Spatial Working Memory in Humans Depends on Theta and High Gamma Synchronization in the Prefrontal Cortex. Curr Biol 26:1513–1521.

Antonakakis M, Dimitriadis SI, Zervakis M, Micheloyannis S, Rezaie R, Babajani-Feremi A, Zouridakis G, Papanicolaou AC (2016) Altered cross-frequency coupling in resting-state MEG after mild traumatic brain injury. Int J Psychophysiol 102:1–11.

Bailey NW, Rogasch NC, Hoy KE, Maller JJ, Rebecca A, Sullivan CM, Fitzgerald PB, Bailey NW, Rogasch NC, Hoy KE, Maller JJ, Segrave A, Sullivan CM, Fitzgerald PB (2017) Increased gamma connectivity during working memory retention following traumatic brain injury. Brain Inj 00:1–11.

Benedict RHB, Groninger L, Schretlen D, Dobraski M, Shpritz B (1996) Revision of the brief visuospatial memory test: Studies of normal performance, reliability, and, validity. Psychol Assess 8:145–153.

Benwell CSY, Davila-Pérez P, Fried PJ, Jones RN, Travison TG, Santarnecchi E, Pascual-Leone A, Shafi MM (2020) EEG spectral power abnormalities and their relationship with cognitive dysfunction in patients with Alzheimer's disease and type 2 diabetes. Neurobiol Aging 85:83–95.

Cassidy JM, Wodeyar A, Wu J, Kaur K, Masuda AK, Srinivasan R, Cramer SC (2020) Low-Frequency Oscillations Are a Biomarker of Injury and Recovery after Stroke. Stroke:1442–1450.

Castellanos NP, Paúl N, Ordóñez VE, Demuynck O, Bajo R, Campo P, Bilbao A, Ortiz T, del-Pozo F, Maestú F (2010) Reorganization of functional connectivity as a correlate of cognitive recovery in acquired brain injury. Brain 133:2365–2381.

Claassen J, Hirsch LJ, Kreiter KT, Du EY, Sander Connolly E, Emerson RG, Mayer SA (2004) Quantitative continuous EEG for detecting delayed cerebral ischemia in patients with poor-grade subarachnoid hemorrhage. Clin Neurophysiol 115:2699–2710.

Collins P, Roberts AC, Dias R, Everitt BJ, Robbins TW (1998) Perseveration and strategy in a novel spatial self-ordered sequencing task for nonhuman primates: Effects of excitotoxic lesions and dopamine depletions of the prefrontal cortex. J Cogn Neurosci 10:332–354.

Corsi PM (1973) Human memory and the medial region of the brain.

Daume J, Gruber T, Engel AK, Friese U (2017) Phase-amplitude coupling and long-range phase synchronization reveal frontotemporal interactions during visual working memory. J Neurosci 37:313–322.

De Simoni S, Grover PJ, Jenkins PO, Honeyfield L, Quest RA, Ross E, Scott G, Wilson MH, Majewska P, Waldman AD, Patel MC, Sharp DJ (2016) Disconnection between the default mode network and medial temporal lobes in post-traumatic amnesia. Brain:1–14.

Della Sala S, Parra MA, Fabi K, Luzzi S, Abrahams S (2012) Short-term memory binding is impaired in AD but not in non-AD dementias. Neuropsychologia 50:833–840.

Fagerholm ED, Scott G, Shew WL, Song C, Leech R, Kn??pfel T, Sharp DJ (2016) Cortical Entropy, Mutual Information and Scale-Free Dynamics in Waking Mice. Cereb Cortex 26:3945–3952.

Fell J, Axmacher N (2011) The role of phase synchronization in memory processes. Nat Rev Neurosci 12:105–118.

Finnigan S, Wong A, Read S (2016) Defining abnormal slow EEG activity in acute ischaemic stroke: Delta/alpha ratio as an optimal QEEG index. Clin Neurophysiol 127:1452–1459.

Friedland D, Swash M (2016) Post-traumatic amnesia and confusional state: hazards of retrospective assessment. J Neurol Neurosurg Psychiatry 87:1068–1074.

Friese U, Köster M, Hassler U, Martens U, Trujillo-Barreto N, Gruber T (2013) Successful memory encoding is associated with increased cross-frequency coupling between frontal theta and posterior gamma oscillations in human scalp-recorded EEG. Neuroimage 66:642–647.

Gabard-Durnam LJ, Leal ASM, Wilkinson CL, Levin AR, Mendez Leal AS, Wilkinson CL, Levin AR (2018)

The Harvard Automated Processing Pipeline for Electroencephalography (HAPPE): Standardized Processing Software for Developmental and High-Artifact Data . Frontiers Media S.A.

Gould RL, Brown RG, Owen AM, Bullmore ET, Williams SCR, Howard RJ (2005) Functional neuroanatomy of successful paired associate learning in Alzheimer's disease. Am J Psychiatry 162:2049–2060.

Grogan JP, Husain M, Manohar SG, Fallon SJ, Zokaei N, Husain M, Zokaei N, Manohar SG, Coulthard EJ, Coulthard EJ (2020) A new toolbox to distinguish the sources of spatial memory error. J Vis 20:1–19.

Hacker CD, Snyder AZ, Pahwa M, Corbetta M, Leuthardt EC (2017) Frequency-specific electrophysiologic correlates of resting state fMRI networks. Neuroimage 149:446–457.

Hampshire A, Highfield RR, Parkin BL, Owen AM (2012) Fractionating Human Intelligence. Neuron 76:1225–1237.

Hennessy MJ, Delle Baite L, Marshman LAG (2021) More than amnesia: prospective cohort study of an integrated novel assessment of the cognitive and behavioural features of PTA. Brain Impair:1–18.

Howells FM, Temmingh HS, Hsieh JH, Van Dijen A V., Baldwin DS, Stein DJ (2018) Electroencephalographic delta/alpha frequency activity differentiates psychotic disorders: A study of schizophrenia, bipolar disorder and methamphetamine-induced psychotic disorder. Transl Psychiatry 8:75.

Huang MX et al. (2014) Single-subject-based whole-brain MEG slow-wave imaging approach for detecting abnormality in patients with mild traumatic brain injury. NeuroImage Clin 5:109–119.

Inoue S, Matsuzawa T (2007) Working memory of numerals in chimpanzees. Curr Biol 17:R1004–R1005.

Jafari Z, Kolb BE, Mohajerani MH (2020) Neural oscillations and brain stimulation in Alzheimer's disease. Prog Neurobiol 194:101878.

Jann K, Kottlow M, Dierks T, Boesch C, Koenig T (2010) Topographic electrophysiological signatures of fMRI resting state networks. PLoS One 5:1–10.

Köster M, Finger H, Graetz S, Kater M, Gruber T (2018) Theta-gamma coupling binds visual perceptual features in an associative memory task. Sci Rep 8.

Kumar S, Rao SL, Chandramouli BA, Pillai S V. (2009) Reduction of functional brain connectivity in mild traumatic brain injury during working memory. J Neurotrauma 26:665–675.

Lega B, Burke J, Jacobs J, Kahana MJ (2016) Slow-Theta-to-Gamma Phase-Amplitude Coupling in Human Hippocampus Supports the Formation of New Episodic Memories. Cereb Cortex 26:268–278.

Leon-Carrion J, Martin-Rodriguez JF, Damas-Lopez J, Barroso y Martin JM, Dominguez-Morales MR (2009) Delta-alpha ratio correlates with level of recovery after neurorehabilitation in patients with acquired brain injury. Clin Neurophysiol 120:1039–1045.

Liang Y, Pertzov Y, Nicholas JM, Henley SMD, Crutch S, Woodward F, Leung K, Fox NC, Husain M (2016) Visual short-term memory binding deficit in familial Alzheimer's disease ScienceDirect.

Luo W, Guan J-S (2018) Do Brain Oscillations Orchestrate Memory? Brain Sci Adv 4:16–33.

Malec JF, Brown AW, Leibson CL, Flaada JT, Mandrekar JN, Diehl NN, Perkins PK (2007) The Mayo Classification System for Traumatic Brain Injury Severity. J Neurotrauma 24:1417–1424.

Maris E, Oostenveld R (2007) Nonparametric statistical testing of EEG- and MEG-data. J Neurosci Methods 164:177–190.

Marshman LAGG, Jakabek D, Hennessy M, Quirk F, Guazzo EP (2013) Post-traumatic amnesia. J Clin Neurosci 20:1475–1481.

McMillan TM (2015) Post Traumatic Amnesia, Second Edi. Elsevier.

Modarres MH, Kuzma NN, Kretzmer T, Pack AI, Lim MM (2017) EEG slow waves in traumatic brain injury: Convergent findings in mouse and man. Neurobiol Sleep Circadian Rhythm 2:59–70.

Mullen T (2012) NITRC: CleanLine: Tool/Resource Info. NITRC CleanLine Tool/Resource Info.

Oostenveld R, Fries P, Maris E, Schoffelen JM (2011) FieldTrip: Open source software for advanced analysis of

MEG, EEG, and invasive electrophysiological data. Comput Intell Neurosci.

Parra MA, Abrahams S, Logie RH, Méndez LG, Lopera F, Della Sala S (2010) Visual short-term memory binding deficits in familial Alzheimer's disease. Brain 133:2702–2713.

Parra MA, Saarimäki H, Bastin ME, Londoño AC, Pettit L, Lopera F, Della Sala S, Abrahams S (2015) Memory binding and white matter integrity in familial Alzheimer's disease. Brain 138:1355–1369.

Pertzov Y, Dong MY, Peich MC, Husain M (2012) Forgetting What Was Where: The Fragility of Object-Location Binding. PLoS One 7.

Ponsford J, Spitz G, McKenzie D (2015) Using Post-Traumatic Amnesia To Predict Outcome after Traumatic Brain Injury. J neurotrauma Epub ahead:1–8.

Robb Swan A, Nichols S, Drake A, Angeles AM, Diwakar M, Song T, Lee RR, Huang MX (2015) Magnetoencephalography slow-wave detection in patients with mild traumatic brain injury and ongoing symptoms correlated with long-term neuropsychological outcome. J Neurotrauma 32:1510–1521.

Schleiger E, Sheikh N, Rowland T, Wong A, Read S, Finnigan S (2014) Frontal EEG delta/alpha ratio and screening for post-stroke cognitive deficits: The power of four electrodes. Int J Psychophysiol 94:19–24.

Schneegans S, Bays PM (2018) New perspectives on binding in visual working memory. :1–38.

Scott G, Fagerholm ED, Mutoh H, Leech R, Sharp DJ, Shew WL, Knopfel T (2014) Voltage Imaging of Waking Mouse Cortex Reveals Emergence of Critical Neuronal Dynamics. J Neurosci 34:16611–16620.

Shores EA, Marosszeky JE, Sandanam J, Batchelor J (1986) Preliminary validation of a clinical scale for measuring the duration of post-traumatic amnesia. Med J Aust 144:569–572.

Sprott JC (1996) Strange attractor symmetric icons. Comput Graph 20:325–332.

Stam CJ, Nolte G, Daffertshofer A (2007) Phase lag index: Assessment of functional connectivity from multi channel EEG and MEG with diminished bias from common sources. Hum Brain Mapp.

Tort ABL, Komorowski R, Eichenbaum H, Kopell N (2010) Measuring phase-amplitude coupling between neuronal oscillations of different frequencies. J Neurophysiol 104:1195–1210.

Tort ABL, Komorowski RW, Manns JR, Kopell NJ, Eichenbaum H (2009) Theta-gamma coupling increases during the learning of item-context associations. Proc Natl Acad Sci U S A 106:20942–20947.

Treisman AM, Gelade G (1980) A feature-integration theory of attention. Cogn Psychol 12:97–136.

Ulam F, Shelton C, Richards L, Davis L, Hunter B, Fregni F, Higgins K (2015) Cumulative effects of transcranial direct current stimulation on EEG oscillations and attention/working memory during subacute neurorehabilitation of traumatic brain injury. Clin Neurophysiol 126:486–496.

Vinck M, Oostenveld R, Van Wingerden M, Battaglia F, Pennartz CMA (2011) An improved index of phase-synchronization for electrophysiological data in the presence of volume-conduction, noise and sample-size bias. Neuroimage.

Vlahou EL, Thurm F, Kolassa IT, Schlee W (2014) Resting-state slow wave power, healthy aging and cognitive performance. Sci Rep 4:1–6.

Wang C, Costanzo ME, Rapp PE, Darmon D, Nathan DE, Bashirelahi K, Pham DL, Roy MJ, Keyser DO (2017) Disrupted gamma synchrony after mild traumatic brain injury and its correlation with white matter abnormality. Front Neurol 8:571.

Wechsler D (1997) Wechsler memory scale (WMS-III). Psychological corporation San Antonio, TX.

Winkler I, Haufe S, Tangermann M (2011) Automatic Classification of Artifactual ICA-Components for Artifact Removal in EEG Signals. Behav Brain Funct 7:30.

Yuan H, Zotev V, Phillips R, Drevets WC, Bodurka J (2012) Spatiotemporal dynamics of the brain at rest - Exploring EEG microstates as electrophysiological signatures of BOLD resting state networks. Neuroimage 60:2062–2072.

Zalesky A, Fornito A, Bullmore ET (2010) Network-based statistic: Identifying differences in brain networks. Neuroimage 53:1197–1207.

Figures & Legends

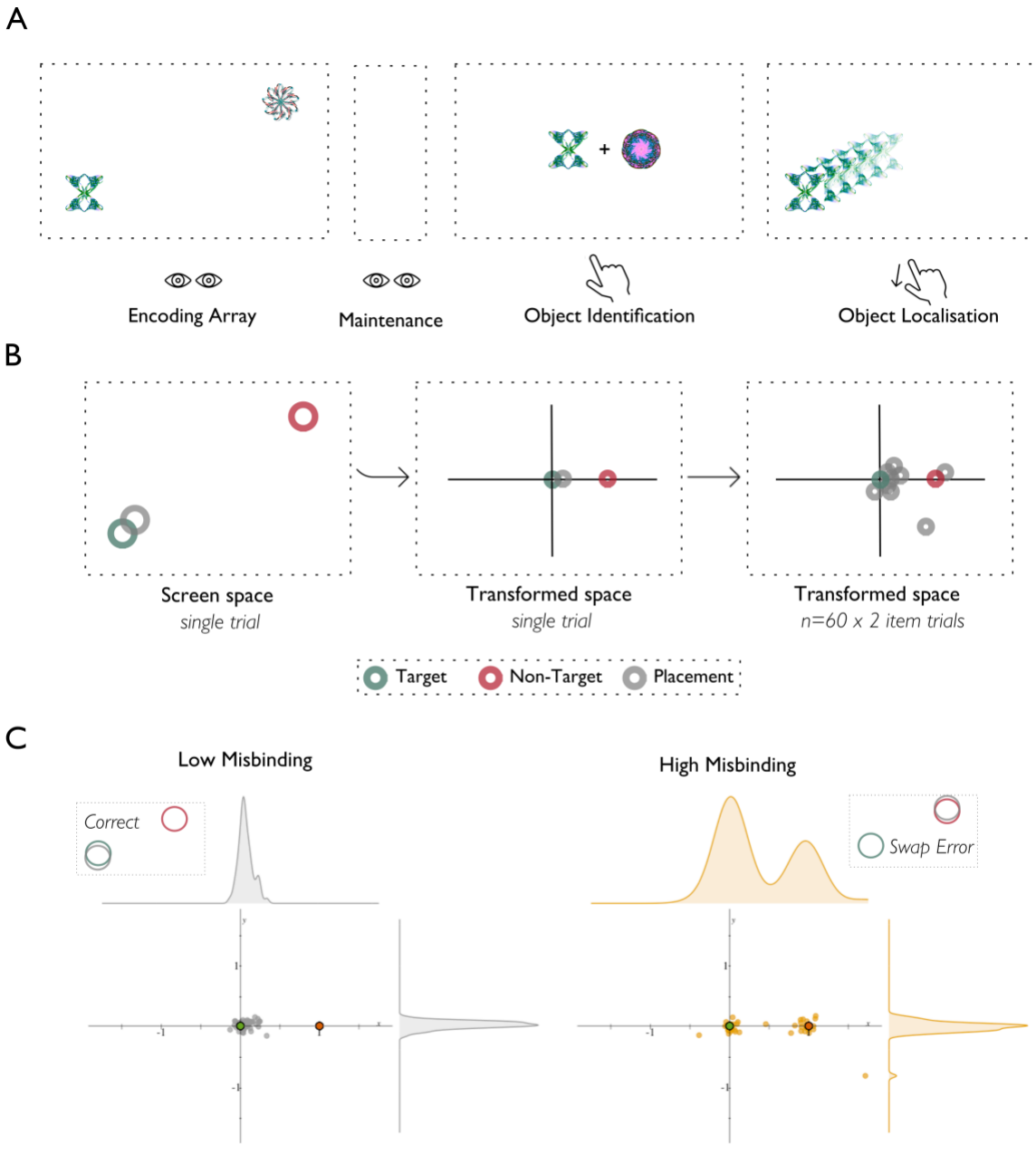

Figure 1. Precision working memory task. (A) Experimental task paradigm. One or two fractal objects are shown ('Encoding Array') prior to a delay of 2 seconds ('Maintenance'). One of the original objects (Target) is then displayed alongside a novel object (Non-Target), which had not appeared in the encoding array. Participants are required to select the object they recall ('Object Identification') and move it to its remembered location ('Object Localisation'). **(B)** Transformation of data from screen space to transformed space in which the target lies at the origin, the non-target at 1,0 (x, y) and the object placement for each trial is plotted in relation to these constants. **(C)** The placements across all trials are visualised using the distribution of responses across the x and y axes in the normalised space. Responses clustered around the target indicate correct responses and-a second cluster around the non-target indicate misbinding errors.

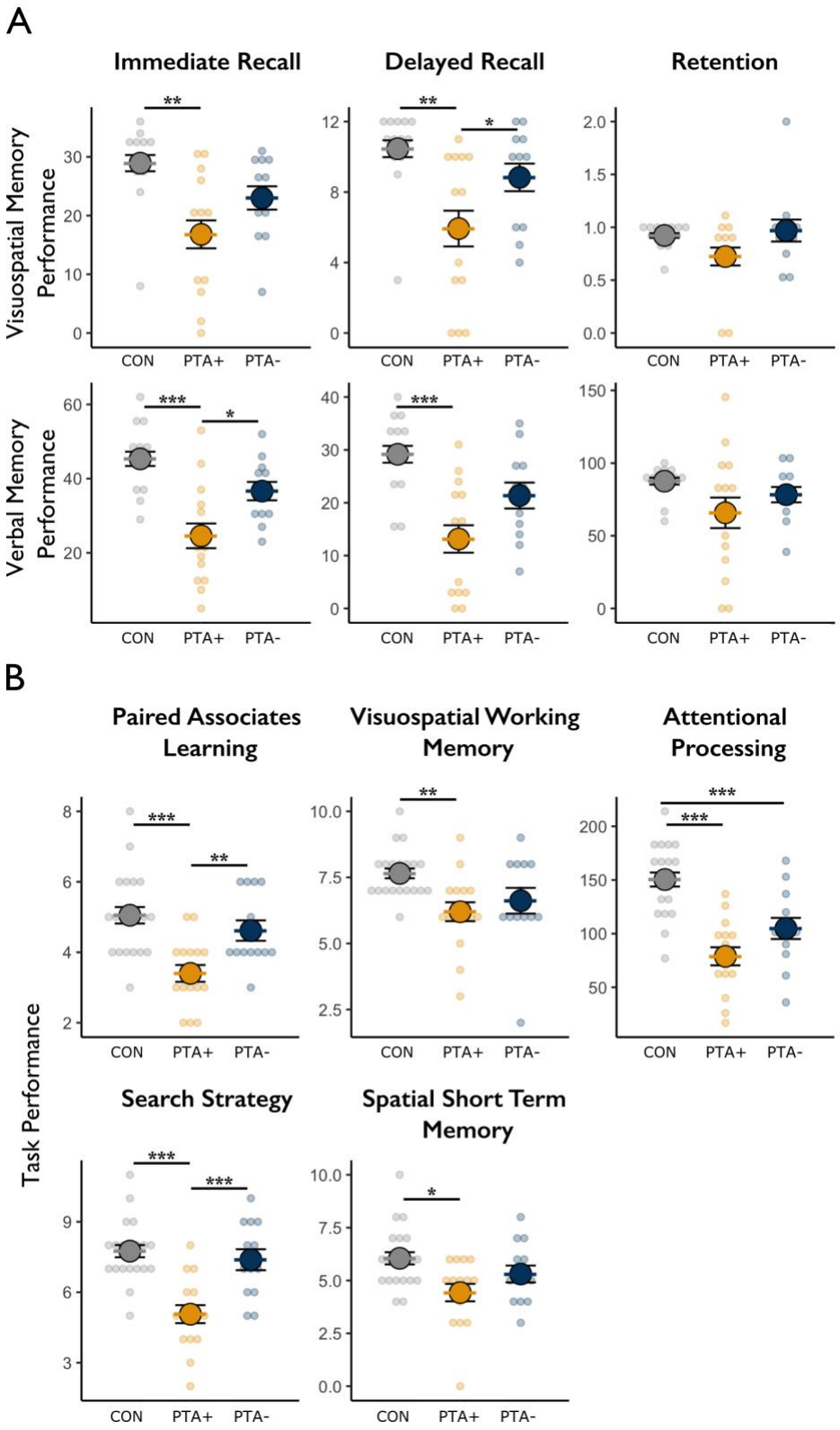

Figure 2. Neuropsychological performance of PTA+ and PTA- TBI patients and healthy controls at baseline. (A) Visuospatial memory performance as measured using the BVMT (top row) and verbal memory performance as measured using the Logical Memory test (bottom row) for immediate recall, delayed recall, and retention. (B) Performance on the computerised battery of tests on the paired associates learning, visuospatial working memory, attentional processing, search strategy and spatial short term memory tasks.

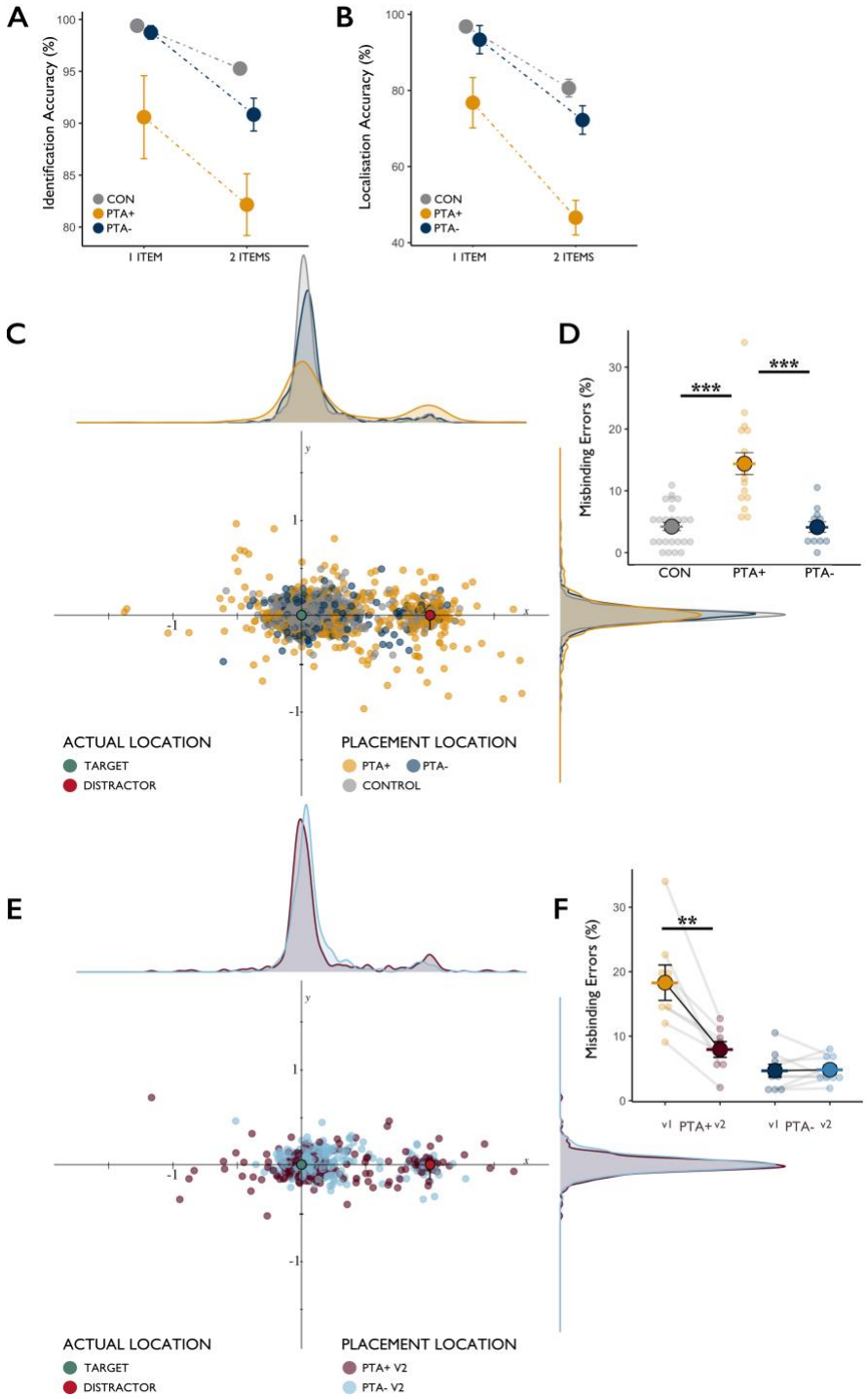

Figure 3. **Performance on the object-location association precision working memory task in healthy controls and PTA+ and PTA- TBI patients at baseline and follow-up. (A)** Object identification accuracy at baseline for 1 and 2 item trials. **(B)** Percentage of correctly identified trials that were moved to the correct location in 1 and 2 item trials at baseline. **(C)** Scatter-hist showing the distribution of location responses correctly identified trials in a normalised space in reference to the target and non-target locations at baseline. **(D)** Percentage of correctly identified trials that resulted in a misbinding error at baseline. **(E)** Scatter-hist showing the distribution of location responses for PTA+ and PTA- TBI patients that returned for follow-up. **(F)** Proportion of misbinding errors made in correctly identified trials by PTA+ and PTA- patients at baseline and follow-up. ***Significance at $P < 0.001$; ** significance at $P < 0.01$; * significance at $P < 0.05$. Error bars represent the standard error of the mean (SEM). CON = healthy controls.

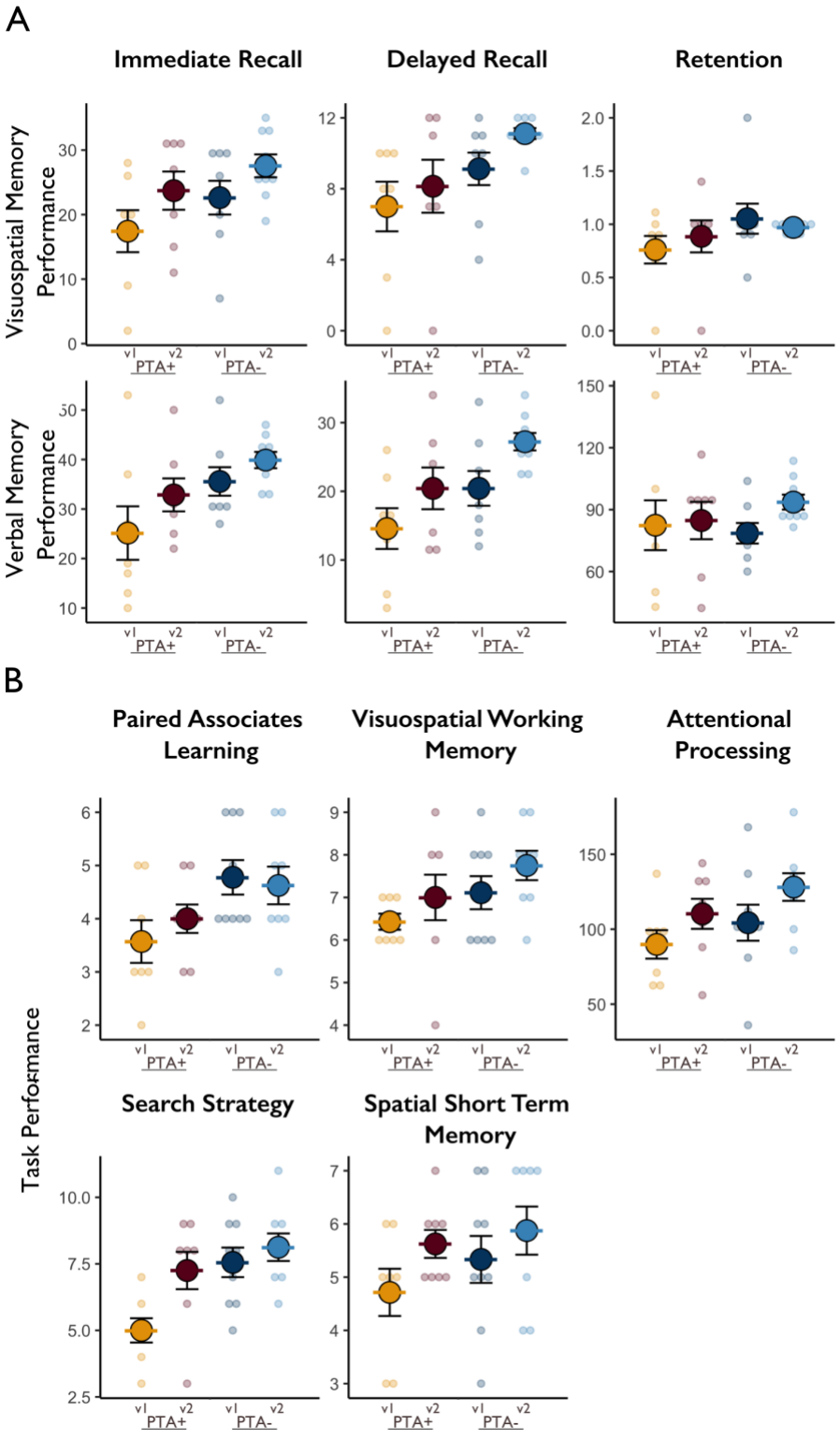

Figure 4. Neuropsychological performance of PTA+ and PTA- TBI patients who returned for follow-up at visit 1 and visit 2. (A) Visuospatial memory performance as measured using the BVMT (top row) and verbal memory performance as measured using the Logical Memory test (bottom row) for immediate recall, delayed recall, and retention. **(B)** Performance on the computerised battery of tests on the paired associates learning, visuospatial working memory, attentional processing, search strategy and spatial short term memory tasks.

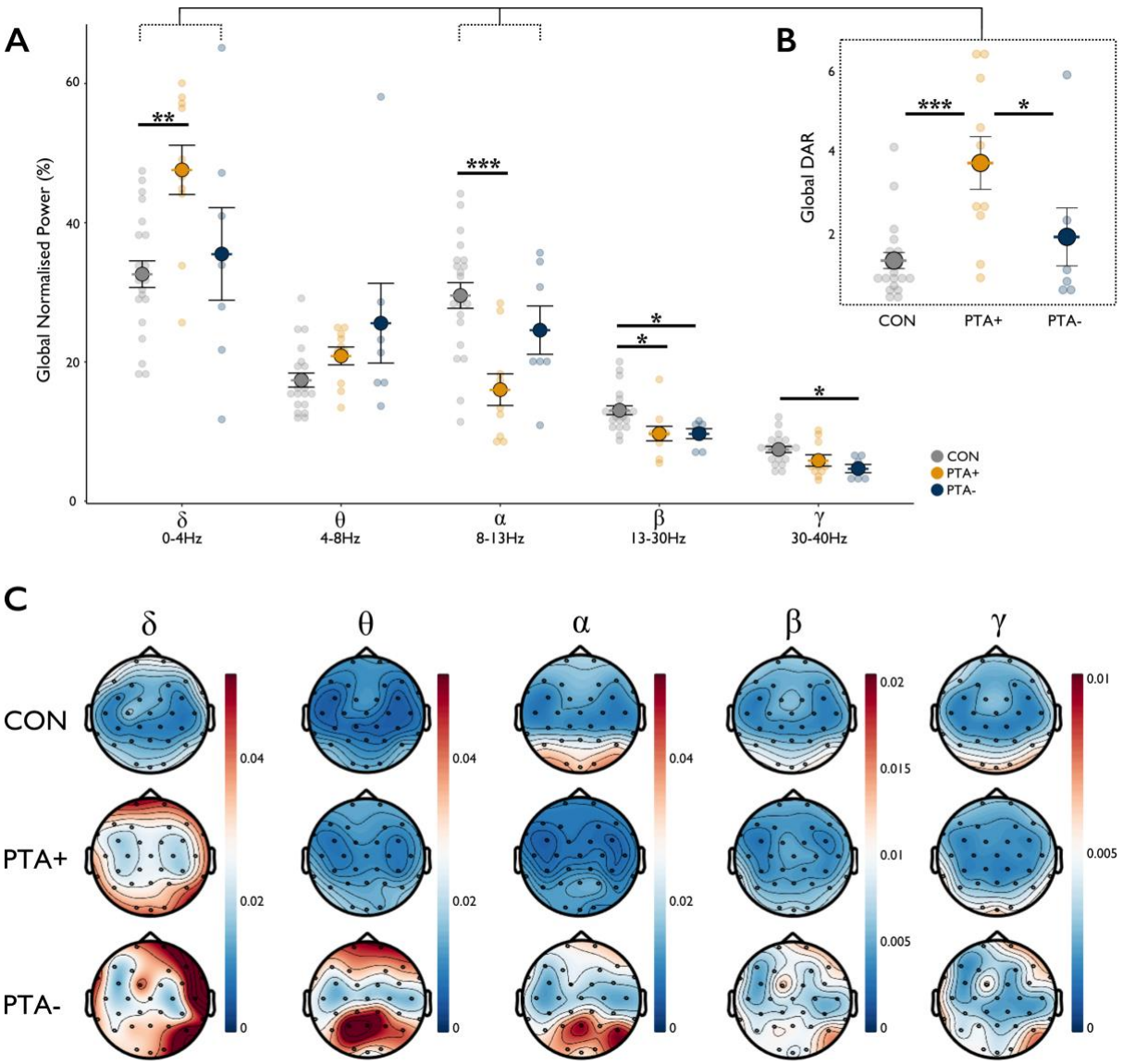

Figure 5. Global normalised power in healthy controls, PTA+ and PTA- TBI patients at baseline. (A) Mean global normalised power for all groups across all frequency bands **(B)** Global delta to alpha ratio across all groups **(C)** Topoplots depicting mean distribution of power for (top to bottom) healthy controls, PTA+, and PTA- groups in (left to right) delta, theta, alpha, beta, and gamma frequency bands. Blue denotes low power; red denotes higher power.

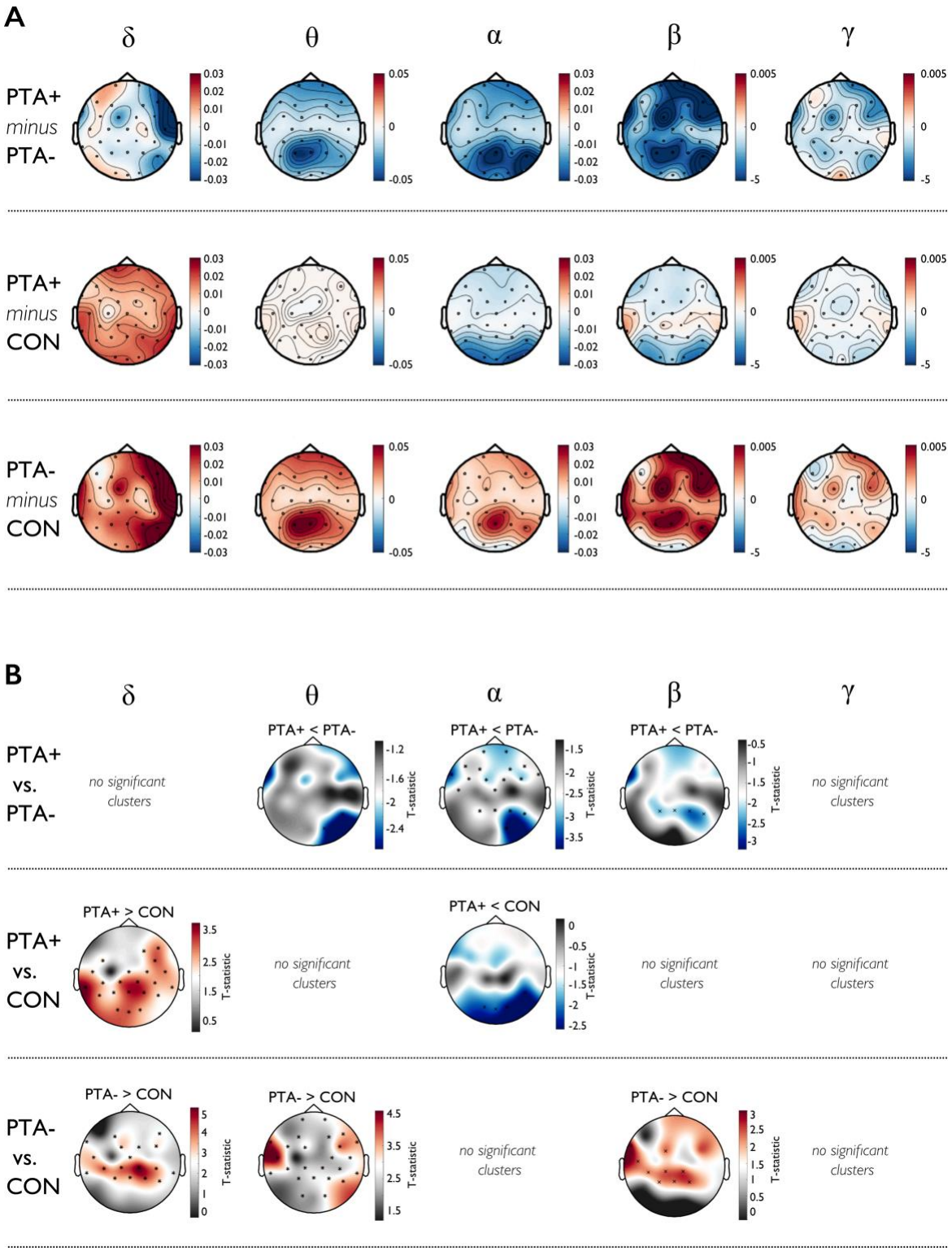

Figure 6. Contrasts in normalised power between healthy controls, PTA+ and PTA- TBI patients at baseline. (A) Absolute differences in power across each channel displayed as raw contrasts for (left to right) delta, theta, alpha, beta, and gamma frequency bands between (top to bottom) PTA+ and PTA-, PTA+ and healthy controls, and PTA- and healthy controls **(B)** Cluster based statistical comparisons of power in (left to right) delta, theta, alpha and beta frequency bands between (top to bottom) PTA+ and PTA-, PTA+ and healthy controls, and PTA- and healthy controls. Areas of red show significant clusters ($P < 0.05$) where power is increased. Areas of blue show significant clusters where power is decreased.

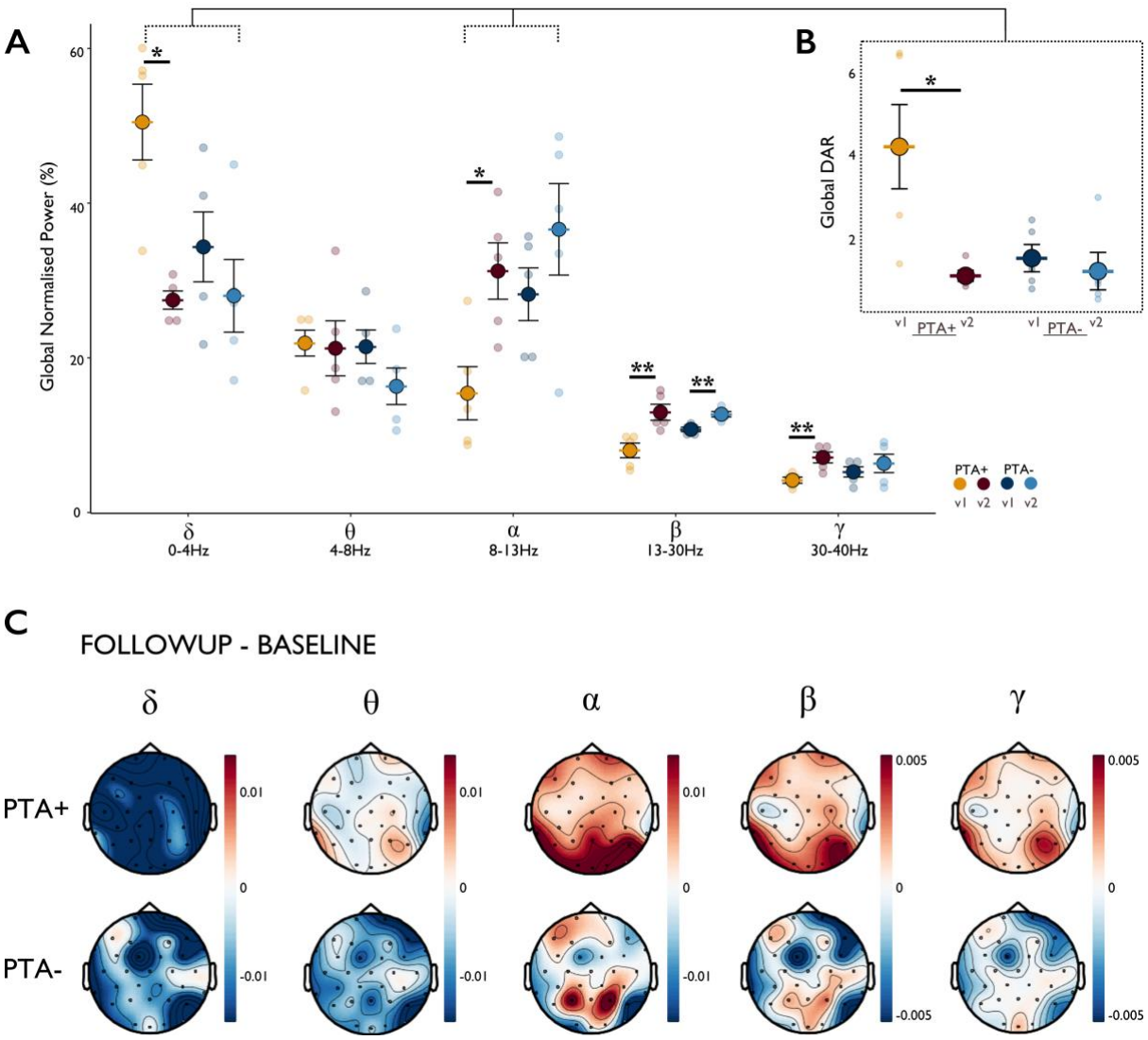

Figure 7. Global normalised power in PTA+ patients and PTA- TBI patients at follow-up. (A) Mean global normalised power for all patients with baseline and follow-up across all frequency bands. **(B)** Global delta to alpha ratio at baseline and follow-up in PTA+ and PTA- TBI patients. **(C)** Topoplots showing change between baseline and follow-up (follow-up minus baseline raw contrast) in PTA+ and PTA- TBI patients in power across all frequency bands. Blue denotes absolute reduction in power at follow-up from baseline, white denotes no change, red denotes absolute increase in power at follow-up from baseline.

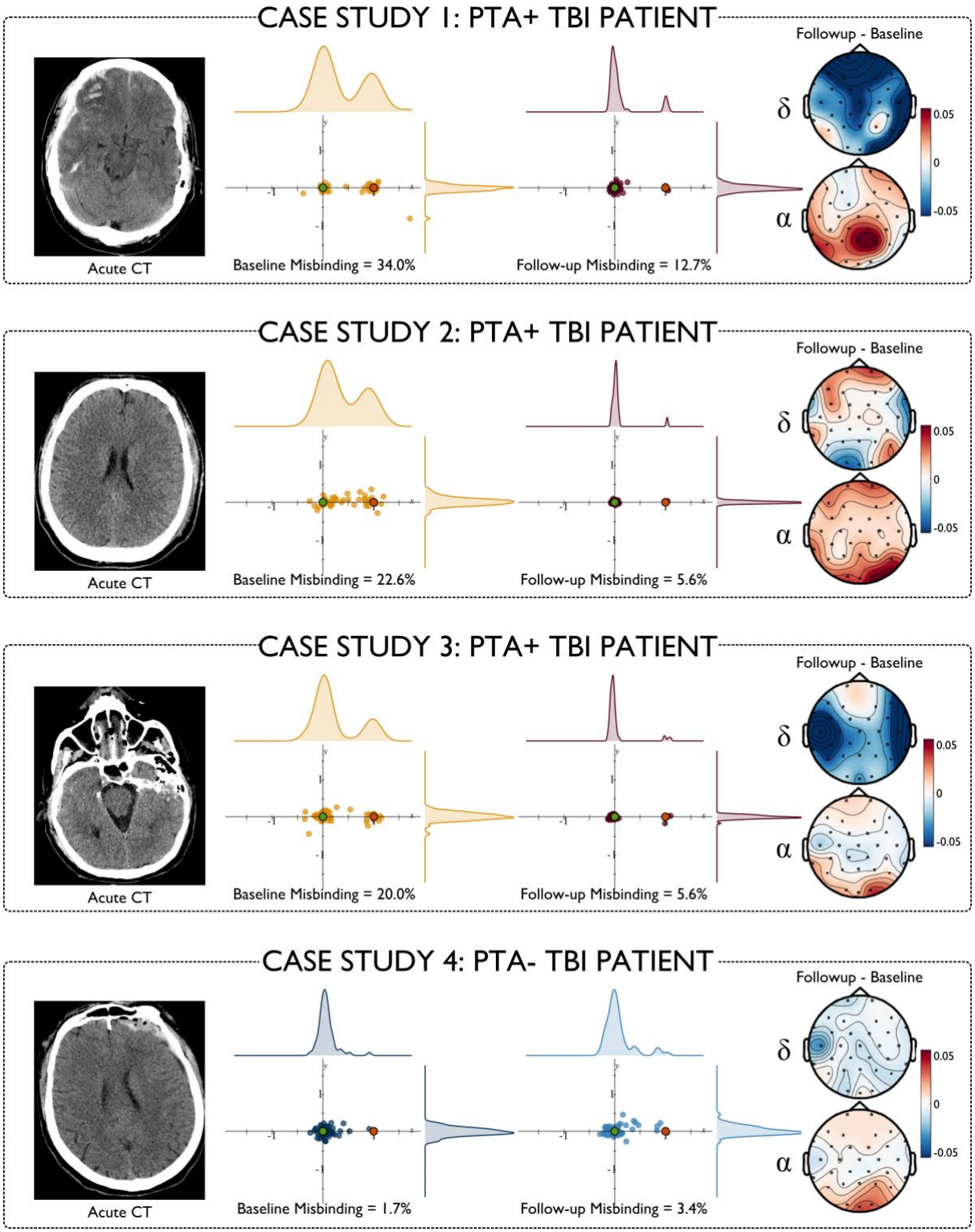

Figure 8. **Individual case studies.** CT head scans at admission are shown on the far left of each case study panel. The distribution of responses in correctly identified trials in the precision spatial working memory task are shown for baseline and follow-up in the middle panels. Topoplots (right) depict changes in delta (top) and alpha (bottom) between baseline and follow-up.

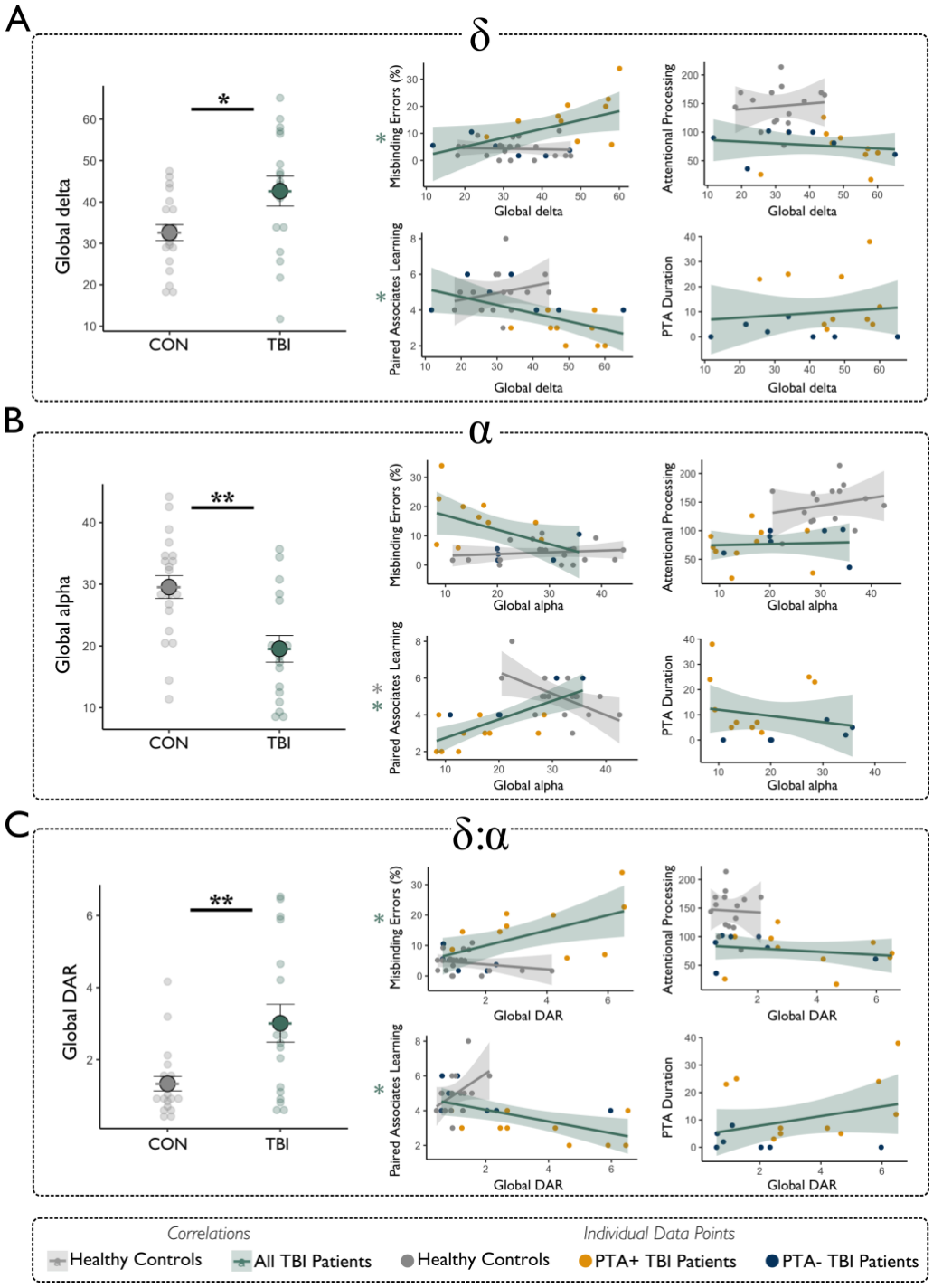

Figure 9. Relationship between global normalised power and cognitive impairment. (A) Global delta power was increased in the TBI group compared to healthy controls and correlated with proportion of misbinding errors and performance on the paired associates learning task. **(B)** Global alpha was significantly decreased in TBI patients compared to healthy controls, and significantly correlated with the performance on the paired associates learning task. **(C)** Global DAR was significantly increased in TBI patients compared to healthy controls and correlated with the proportion of misbinding errors, and performance on the paired associates learning task.

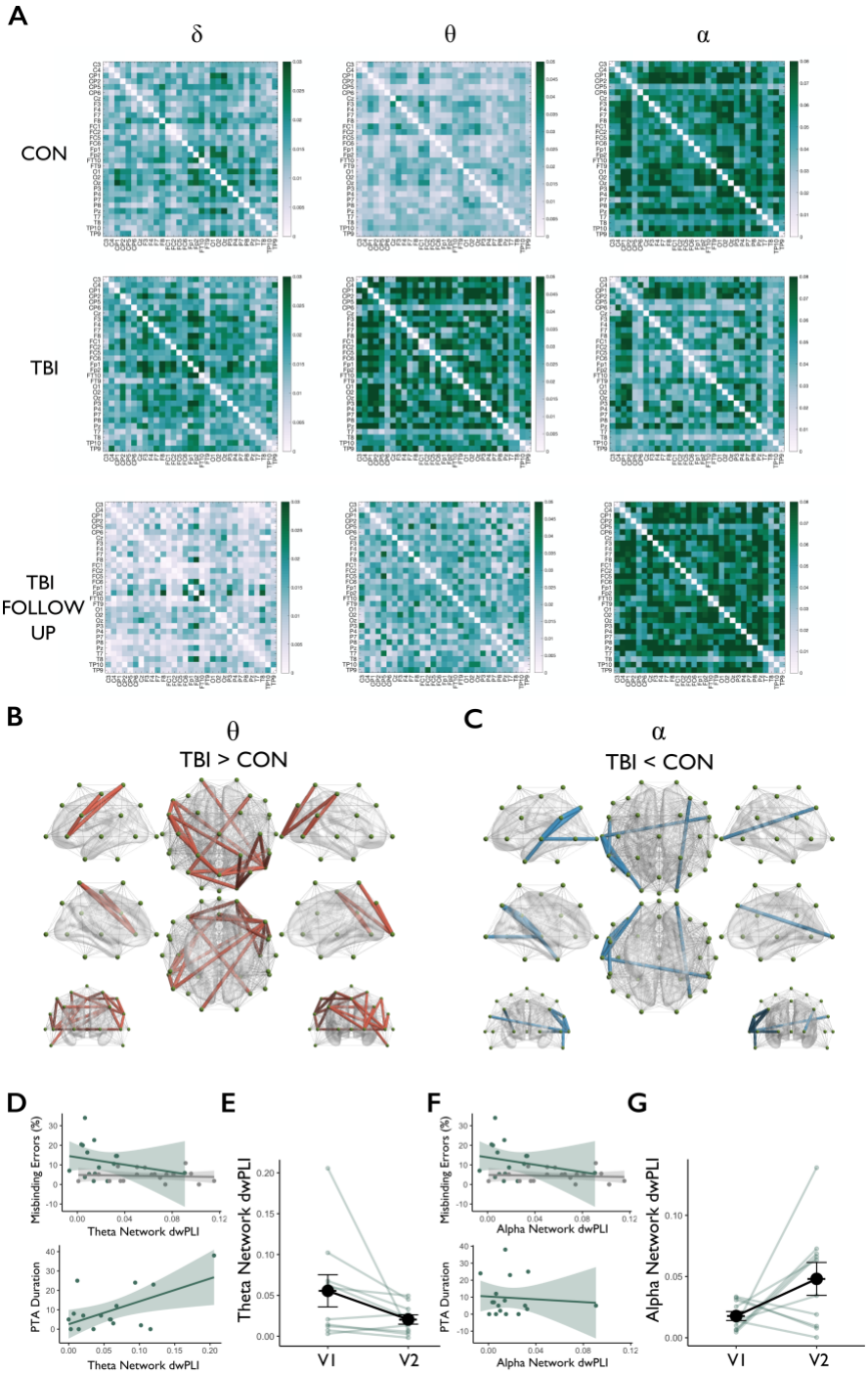

Figure 10. Phase synchronisation. (A) Whole brain connectivity matrices in delta, theta and alpha frequency bands for healthy controls (top row), all TBI patients at baseline (middle row) and all TBI patients returning for follow-up (bottom row) **(B)** Network based statistics revealed one robust network of hyperconnectivity in TBI patients at baseline compared to controls in the theta band and **(C)** one robust network of hypoconnectivity in the alpha band. **(D)** Mean dwPLI in the resulting theta network was positively associated with total PTA duration but showed no relationship to misbinding errors in patients or controls **(E)** Mean dwpLI in the theta network in patients at baseline and follow-up. **(F)** Mean dwpLI in the resulting alpha network showed no relationship between misbinding errors in patients or controls or to PTA duration. **(G)** Mean dwpLI in the alpha network in patients at baseline and follow-up.

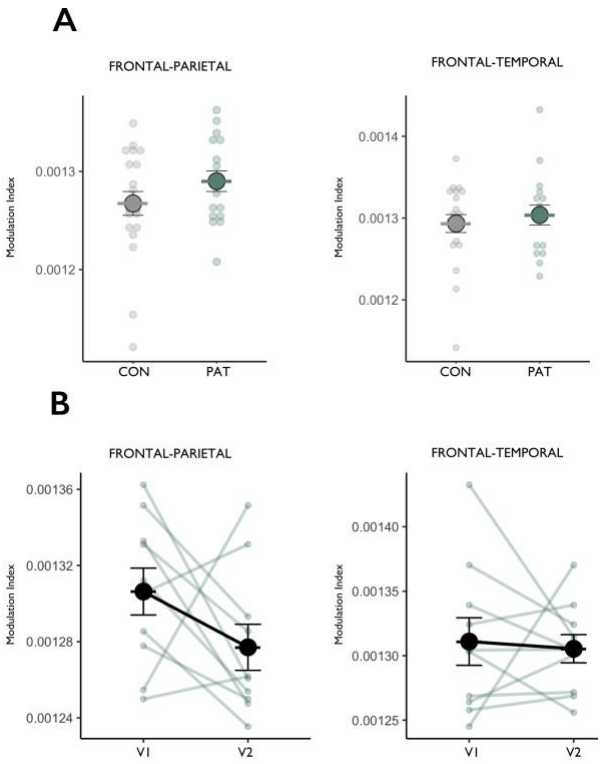

Figure 11. Frontal theta phase to parietal and temporal gamma amplitude coupling. (A) Average modulation index between frontal and parietal channels (left) and frontal and temporal channels (right) in all TBI patients (PAT) and controls at baseline. **(B)** Longitudinal changes in phase-amplitude coupling between frontal-parietal (left) and frontal-temporal (right) channels in patients at follow-up. Error bars represent standard error of the mean.